Sports, and Culture of Japan. We thank Dr. Yasuko Nishizawa for advice with immunohistochemistry.

■ ABBREVIATIONS

iTRAQ, isobaric peptide tags for relative and absolute quantification; SRM, selected reaction monitoring; MRM, multiple reaction monitoring; PTS, phase-transfer surfactants; SI-peptide, stable isotope-labeled peptide; CID, collision-induced dissociation; HCD, higher energy collision-induced dissociation; IHC, Immunohistochemistry; LC–MS/MS, liquid chromatography tandem mass spectrometry; CE, Collision energy; LTQ, linear ion trap; fwhm, full wide at half maximum; FDR, false discovery rate.

■ REFERENCES

(1) Zeng, G. Q.; Zhang, P. F.; Deng, X. M.; Yu, F. L.; Li, C.; Xu, Y.; Yi, H.; Li, M. Y.; Hu, R.; Zuo, J. H.; Li, X. H.; Wan, X. X.; Qu, J. Q.; He, Q. Y.; Li, J. H.; Ye, X.; Chen, Y.; Li, J. Y.; Xiao, Z. Q. Identification of candidate biomarkers for early detection of human lung squamous cell cancer by quantitative proteomics. *Mol. Cell. Proteomics* **2012**, *11* (6), M111013946.

(2) Ghosh, D.; Yu, H.; Tan, X. F.; Lim, T. K.; Zubaidah, R. M.; Tan, H. T.; Chung, M. C.; Lin, Q. Identification of key players for colorectal cancer metastasis by iTRAQ quantitative proteomics profiling of isogenic SW480 and SW620 cell lines. *J. Proteome Res.* **2011**, *10* (10), 4373–87.

(3) Li, Z.; Adams, R. M.; Chourey, K.; Hurst, G. B.; Hettich, R. L.; Pan, C. Systematic comparison of label-free, metabolic labeling, and isobaric chemical labeling for quantitative proteomics on LTQ Orbitrap velos. *J. Proteome Res.* **2012**, *11* (3), 1582–90.

(4) Gygi, S. P.; Rist, B.; Gerber, S. A.; Turecek, F.; Gelb, M. H.; Aebersold, R. Quantitative analysis of complex protein mixtures using isotope-coded affinity tags. *Nat. Biotechnol.* **1999**, *17* (10), 994–9.

(5) Ross, P. L.; Huang, Y. N.; Marchese, J. N.; Williamson, B.; Parker, K.; Hattan, S.; Khainovski, N.; Pillai, S.; Dey, S.; Daniels, S.; Purkayastha, S.; Juhasz, P.; Martin, S.; Bartlet-Jones, M.; He, F.; Jacobson, A.; Pappin, D. J. Multiplexed protein quantitation in Saccharomyces cerevisiae using amine-reactive isobaric tagging reagents. *Mol. Cell. Proteomics* **2004**, *3* (12), 1154–69.

(6) Collier, T. S.; Sarkar, P.; Franck, W. L.; Rao, B. M.; Dean, R. A.; Muddiman, D. C. Direct comparison of stable isotope labeling by amino acids in cell culture and spectral counting for quantitative proteomics. *Anal. Chem.* **2010**, *82* (20), 8696–702.

(7) Whiteaker, J. R.; Lin, C.; Kennedy, J.; Hou, L.; Trute, M.; Sokal, I.; Yan, P.; Schoenherr, R. M.; Zhao, L.; Voytovich, U. J.; Kelly-Spratt, K. S.; Krasnoselsky, A.; Gafken, P. R.; Hogan, J. M.; Jones, L. A.; Wang, P.; Amon, L.; Chodosh, L. A.; Nelson, P. S.; McIntosh, M. W.; Kemp, C. J.; Paulovich, A. G. A targeted proteomics-based pipeline for verification of biomarkers in plasma. *Nat. Biotechnol.* **2011**, *29* (7), 625–34.

(8) Thingholm, T. E.; Bak, S.; Beck-Nielsen, H.; Jensen, O. N.; Gaster, M. Characterization of human myotubes from type 2 diabetic and nondiabetic subjects using complementary quantitative mass spectrometric methods. *Mol. Cell. Proteomics* **2011**, *10* (9), M110 006650.

(9) Addona, T. A.; Abbatiello, S. E.; Schilling, B.; Skates, S. J.; Mani, D. R.; Bunk, D. M.; Spiegelman, C. H.; Zimmerman, L. J.; Ham, A. J.; Keshishian, H.; Hall, S. C.; Allen, S.; Blackman, R. K.; Borchers, C. H.; Buck, C.; Cardasis, H. L.; Cusack, M. P.; Dodder, N. G.; Gibson, B. W.; Held, J. M.; Hiltke, T.; Jackson, A.; Johansen, E. B.; Kinsinger, C. R.; Li, J.; Mesri, M.; Neubert, T. A.; Niles, R. K.; Pulsipher, T. C.; Ransohoff, D.; Rodriguez, H.; Rudnick, P. A.; Smith, D.; Tabb, D. L.; Tegeler, T. J.; Variyath, A. M.; Vega-Montoto, L. J.; Wahlander, A.; Waldemarson, S.; Wang, M.; Whiteaker, J. R.; Zhao, L.; Anderson, N. L.; Fisher, S. J.; Liebler, D. C.; Paulovich, A. G.; Regnier, F. E.; Tempst, P.; Carr, S. A. Multi-site assessment of the precision and reproducibility of multiple reaction monitoring-based measurements of proteins in plasma. *Nat. Biotechnol.* **2009**, *27* (7), 633–41.

(10) Drabovich, A. P.; Jarvi, K.; Diamandis, E. P. Verification of male infertility biomarkers in seminal plasma by multiplex selected reaction monitoring assay. *Mol. Cell. Proteomics* **2011**, *10* (12), M110 004127.

(11) Yates, J. R., 3rd; Gilchrist, A.; Howell, K. E.; Bergeron, J. J. Proteomics of organelles and large cellular structures. *Nat. Rev. Mol. Cell. Biol.* **2005**, *6* (9), 702–14.

(12) Polisetty, R. V.; Gautam, P.; Sharma, R.; Harsha, H. C.; Nair, S. C.; Gupta, M. K.; Uppin, M. S.; Challa, S.; Puligopu, A. K.; Ankathi, P.; Purohit, A. K.; Chandak, G. R.; Pandey, A.; Sirdeshmukh, R. LC-MS/MS analysis of differentially expressed glioblastoma membrane proteome reveals altered calcium signalling and other protein groups of regulatory functions. *Mol. Cell. Proteomics* **2012**, *11* (6), M111013565.

(13) Josic, D.; Clifton, J. G. Mammalian plasma membrane proteomics. *Proteomics* **2007**, *7* (16), 3010–29.

(14) Russell, W. K.; Park, Z. Y.; Russell, D. H. Proteolysis in mixed organic-aqueous solvent systems: applications for peptide mass mapping using mass spectrometry. *Anal. Chem.* **2001**, *73* (11), 2682–5.

(15) Blonder, J.; Goshe, M. B.; Moore, R. J.; Pasa-Tolic, L.; Masselon, C. D.; Lipton, M. S.; Smith, R. D. Enrichment of integral membrane proteins for proteomic analysis using liquid chromatography-tandem mass spectrometry. *J. Proteome Res.* **2002**, *1* (4), 351–60.

(16) Chick, J. M.; Haynes, P. A.; Molloy, M. P.; Bjellqvist, B.; Baker, M. S.; Len, A. C. Characterization of the rat liver membrane proteome using peptide immobilized pH gradient isoelectric focusing. *J. Proteome Res.* **2008**, *7* (3), 1036–45.

(17) Wu, C. C.; MacCoss, M. J.; Howell, K. E.; Yates, J. R., 3rd A method for the comprehensive proteomic analysis of membrane proteins. *Nat. Biotechnol.* **2003**, *21* (5), 532–8.

(18) Schindler, J.; Lewandrowski, U.; Sickmann, A.; Friauf, E.; Nothwang, H. G. Proteomic analysis of brain plasma membranes isolated by affinity two-phase partitioning. *Mol. Cell. Proteomics* **2006**, *5* (2), 390–400.

(19) Rahbar, A. M.; Fenselau, C. Integration of Jacobson's pellicle method into proteomic strategies for plasma membrane proteins. *J. Proteome Res.* **2004**, *3* (6), 1267–77.

(20) Masuda, T.; Tomita, M.; Ishihama, Y. Phase transfer surfactant-aided trypsin digestion for membrane proteome analysis. *J. Proteome Res.* **2008**, *7* (2), 731–40.

(21) van 't Veer, L. J.; Dai, H.; van de Vijver, M. J.; He, Y. D.; Hart, A. A.; Mao, M.; Peterse, H. L.; van der Kooy, K.; Marton, M. J.; Witteveen, A. T.; Schreiber, G. J.; Kerkhoven, R. M.; Roberts, C.; Linsley, P. S.; Bernards, R.; Friend, S. H. Gene expression profiling predicts clinical outcome of breast cancer. *Nature* **2002**, *415* (6871), 530–6.

(22) Paik, S.; Shak, S.; Tang, G.; Kim, C.; Baker, J.; Cronin, M.; Baehner, F. L.; Walker, M. G.; Watson, D.; Park, T.; Hiller, W.; Fisher, E. R.; Wickerham, D. L.; Bryant, J.; Wolmark, N. A multigene assay to predict recurrence of tamoxifen-treated, node-negative breast cancer. *N. Engl. J. Med.* **2004**, *351* (27), 2817–26.

(23) Cheang, M. C.; Chia, S. K.; Voduc, D.; Gao, D.; Leung, S.; Snider, J.; Watson, M.; Davies, S.; Bernard, P. S.; Parker, J. S.; Perou, C. M.; Ellis, M. J.; Nielsen, T. O. Ki67 index, HER2 status, and prognosis of patients with luminal B breast cancer. *J. Natl. Cancer Inst.* **2009**, *101* (10), 736–50.

(24) Rappsilber, J.; Mann, M.; Ishihama, Y. Protocol for micro-purification, enrichment, pre-fractionation and storage of peptides for proteomics using StageTips. *Nat. Protoc.* **2007**, *2* (8), 1896–906.

(25) Krogh, A.; Larsson, B.; von Heijne, G.; Sonnhammer, E. L. Predicting transmembrane protein topology with a hidden Markov model: application to complete genomes. *J. Mol. Biol.* **2001**, *305* (3), 567–80.

(26) Ishitobi, M.; Goranova, T. E.; Komoike, Y.; Motomura, K.; Koyama, H.; Glas, A. M.; van Lienen, E.; Inaji, H.; Van't Veer, L. J.;

Kato, K. Clinical utility of the 70-gene MammaPrint profile in a Japanese population. *Jpn. J. Clin. Oncol.* **2010**, *40* (6), 508–12.
(27) Soiland, H.; Janssen, E. A.; Korner, H.; Varhaug, J. E.; Skaland, I.; Gudlaugsson, E.; Baak, J. P.; Soreide, J. A. Apolipoprotein D predicts adverse outcome in women >or=70 years with operable breast cancer. *Breast Cancer Res. Treat.* **2009**, *113* (3), 519–28.
(28) Zeng, Z.; Hincapie, M.; Pitteri, S. J.; Hanash, S.; Schalkwijk, J.; Hogan, J. M.; Wang, H.; Hancock, W. S. A proteomics platform combining depletion, multi-lectin affinity chromatography (M-LAC), and isoelectric focusing to study the breast cancer proteome. *Anal. Chem.* **2011**, *83* (12), 4845–54.
(29) Hamrita, B.; Chahed, K.; Trimeche, M.; Guillier, C. L.; Hammann, P.; Chaieb, A.; Korbi, S.; Chouchane, L. Proteomics-based identification of alpha1-antitrypsin and haptoglobin precursors as novel serum markers in infiltrating ductal breast carcinomas. *Clin. Chim. Acta* **2009**, *404* (2), 111–8.
(30) Shipp, C.; Watson, K.; Jones, G. L. Associations of HSP90 client proteins in human breast cancer. *Anticancer Res.* **2011**, *31* (6), 2095–101.
(31) Pupa, S. M.; Argraves, W. S.; Forti, S.; Casalini, P.; Berno, V.; Agresti, R.; Aiello, P.; Invernizzi, A.; Baldassari, P.; Twal, W. O.; Mortarini, R.; Anichini, A.; Menard, S. Immunological and pathobiological roles of fibulin-1 in breast cancer. *Oncogene* **2004**, *23* (12), 2153–60.
(32) Lee, Y. H.; Albig, A. R.; Regner, M.; Schiemann, B. J.; Schiemann, W. P. Fibulin-5 initiates epithelial-mesenchymal transition (EMT) and enhances EMT induced by TGF-beta in mammary epithelial cells via a MMP-dependent mechanism. *Carcinogenesis* **2008**, *29* (12), 2243–51.
(33) Freije, J. P.; Fueyo, A.; Uria, J.; Lopez-Otin, C. Human Zn-alpha 2-glycoprotein cDNA cloning and expression analysis in benign and malignant breast tissues. *FEBS Lett.* **1991**, *290* (1–2), 247–9.
(34) Baniwal, S. K.; Little, G. H.; Chimge, N. O.; Frenkel, B. Runx2 controls a feed-forward loop between androgen and prolactin-induced protein (PIP) in stimulating T47D cell proliferation. *J. Cell Physiol.* **2012**, *227* (5), 2276–82.
(35) Ma, X. J.; Dahiya, S.; Richardson, E.; Erlander, M.; Sgroi, D. C. Gene expression profiling of the tumor microenvironment during breast cancer progression. *Breast Cancer Res.* **2009**, *11* (1), R7.
(36) Joensuu, K.; Heikkila, P.; Andersson, L. C. Tumor dormancy: elevated expression of stanniocalcins in late relapsing breast cancer. *Cancer Lett.* **2008**, *265* (1), 76–83.
(37) Raulic, S.; Ramos-Valdes, Y.; DiMattia, G. E. Stanniocalcin 2 expression is regulated by hormone signalling and negatively affects breast cancer cell viability in vitro. *J. Endocrinol.* **2008**, *197* (3), 517–29.
(38) Culhane, A. C.; Quackenbush, J. Confounding effects in "A six-gene signature predicting breast cancer lung metastasis". *Cancer Res.* **2009**, *69* (18), 7480–5.
(39) Picotti, P.; Rinner, O.; Stallmach, R.; Dautel, F.; Farrah, T.; Domon, B.; Wenschuh, H.; Aebersold, R. High-throughput generation of selected reaction-monitoring assays for proteins and proteomes. *Nat. Methods* **2010**, *7* (1), 43–6.
(40) Chen, J. S.; Chen, K. T.; Fan, C. W.; Han, C. L.; Chen, Y. J.; Yu, J. S.; Chang, Y. S.; Chien, C. W.; Wu, C. P.; Hung, R. P.; Chan, E. C. Comparison of membrane fraction proteomic profiles of normal and cancerous human colorectal tissues with gel-assisted digestion and iTRAQ labeling mass spectrometry. *FEBS J.* **2010**, *277* (14), 3028–38.
(41) Han, C. L.; Chen, J. S.; Chan, E. C.; Wu, C. P.; Yu, K. H.; Chen, K. T.; Tsou, C. C.; Tsai, C. F.; Chien, C. W.; Kuo, Y. B.; Lin, P. Y.; Yu, J. S.; Hsueh, C.; Chen, M. C.; Chan, C. C.; Chang, Y. S.; Chen, Y. J. An informatics-assisted label-free approach for personalized tissue membrane proteomics: case study on colorectal cancer. *Mol. Cell. Proteomics* **2011**, *10* (4), M110 003087.
(42) Iwasaki, M.; Masuda, T.; Tomita, M.; Ishihama, Y. Chemical cleavage-assisted tryptic digestion for membrane proteome analysis. *J. Proteome Res.* **2009**, *8* (6), 3169–75.
(43) Ross, J. S.; Hatzis, C.; Symmans, W. F.; Pusztai, L.; Hortobagyi, G. N. Commercialized multigene predictors of clinical outcome for breast cancer. *Oncologist* **2008**, *13* (5), 477–93.
(44) Goldhirsch, A; Wood, W. C.; Coates, A. S.; Gelber, R. D.; Thurlimann, B; Senn, H. J. Strategies for subtypes--dealing with the diversity of breast cancer: highlights of the St. Gallen International Expert Consensus on the Primary Therapy of Early Breast Cancer 2011. *Ann. Oncol.* **2011**, *22* (8), 1736–47.
(45) Zhao, Z.; Lee, C. C.; Jiralerspong, S.; Juyal, R. C.; Lu, F.; Baldini, A.; Greenberg, F.; Caskey, C. T.; Patel, P. I. The gene for a human microfibril-associated glycoprotein is commonly deleted in Smith-Magenis syndrome patients. *Hum. Mol. Genet.* **1995**, *4* (4), 589–97.
(46) Schlosser, A.; Thomsen, T.; Shipley, J. M.; Hein, P. W.; Brasch, F.; Tornoe, I.; Nielsen, O.; Skjodt, K.; Palaniyar, N.; Steinhilber, W.; McCormack, F. X.; Holmskov, U. Microfibril-associated protein 4 binds to surfactant protein A (SP-A) and colocalizes with SP-A in the extracellular matrix of the lung. *Scand. J. Immunol.* **2006**, *64* (2), 104–16.
(47) Lausen, M.; Lynch, N.; Schlosser, A.; Tornoe, I.; Saekmose, S. G.; Teisner, B.; Willis, A. C.; Crouch, E.; Schwaeble, W.; Holmskov, U. Microfibril-associated protein 4 is present in lung washings and binds to the collagen region of lung surfactant protein D. *J. Biol. Chem.* **1999**, *274* (45), 32234–40.
(48) Toyoshima, T.; Ishida, T.; Nishi, N.; Kobayashi, R.; Nakamura, T.; Itano, T. Differential gene expression of 36-kDa microfibril-associated glycoprotein (MAGP-36/MFAP4) in rat organs. *Cell Tissue Res.* **2008**, *332* (2), 271–8.
(49) MacDonald, R. J.; Ronzio, R. A. Comparative analysis of zymogen granule membrane polypeptides. *Biochem. Biophys. Res. Commun.* **1972**, *49* (2), 377–82.
(50) Ronzio, R. A.; Kronquist, K. E.; Lewis, D. S.; MacDonald, R. J.; Mohrlok, S. H.; O'Donnell, J. J., Jr. Glycoprotein synthesis in the adult rat pancreas. IV. Subcellular distribution of membrane glycoproteins. *Biochim. Biophys. Acta* **1978**, *508* (1), 65–84.
(51) Scheele, G. A.; Fukuoka, S.; Freedman, S. D. Role of the GP2/THP family of GPI-anchored proteins in membrane trafficking during regulated exocrine secretion. *Pancreas* **1994**, *9* (2), 139–49.
(52) Hase, K.; Kawano, K.; Nochi, T.; Pontes, G. S.; Fukuda, S.; Ebisawa, M.; Kadokura, K.; Tobe, T.; Fujimura, Y.; Kawano, S.; Yabashi, A.; Waguri, S.; Nakato, G.; Kimura, S.; Murakami, T.; Iimura, M.; Hamura, K.; Fukuoka, S.; Lowe, A. W.; Itoh, K.; Kiyono, H.; Ohno, H. Uptake through glycoprotein 2 of FimH(+) bacteria by M cells initiates mucosal immune response. *Nature* **2009**, *462* (7270), 226–30.

JOURNAL OF PROTEOMICS 75 (2012) 1803–1815

Available online at www.sciencedirect.com

SciVerse ScienceDirect

www.elsevier.com/locate/jprot

Plectin promotes migration and invasion of cancer cells and is a novel prognostic marker for head and neck squamous cell carcinoma

Koji Katada[a], *Takeshi Tomonaga*[b,c,*], *Mamoru Satoh*[c], *Kazuyuki Matsushita*[c], *Yurie Tonoike*[a], *Yoshio Kodera*[d], *Toyoyuki Hanazawa*[a], *Fumio Nomura*[c], *Yoshitaka Okamoto*[a]

[a]*Department of Otorhinolaryngology, Head and Neck Surgery, Graduate School of Medicine, Chiba University, 1-8-1 Inohana, Chuo-ku, Chiba 260–8670, Japan*
[b]*Laboratory of Proteome Research, National Institute of Biomedical Innovation, 7-6-8 Saito-Asagi, Ibaraki 567–0085, Japan*
[c]*Department of Molecular Diagnosis, Graduate School of Medicine, Chiba University, 1-8-1 Inohana, Chuo-ku, Chiba 260–8670, Japan*
[d]*Department of Physics, Laboratory of Biomolecular Dynamics, Kitasato University School of Science, 1-15-1 Kitasato, Sagamihara, Kanagawa 228–8555, Japan*

ARTICLE INFO

Article history:
Received 23 August 2011
Accepted 14 December 2011
Available online 30 December 2011

Keywords:
Head and neck cancer
Plectin
2D-DIGE
Prognostic marker

ABSTRACT

Head and neck squamous cell carcinoma (HNSCC) is usually found at a late stage and distant metastasis occurs at high frequency; therefore, novel prognostic markers are needed. This study was aimed to identify novel tumor markers in HNSCC. We identified 65 proteins which were significantly increased or decreased in the tumors by 2D-DIGE using 12 HNSCC and adjacent non-cancer tissues. Western blotting and immunohistochemical analysis confirmed that the expression of plectin was significantly increased in most cancer tissues as compared with non-cancer tissues. Strikingly, the suppression of endogenous plectin using siRNA inhibited the proliferation, migration and invasion of HNSCC cells and down-regulated Erk 1/2 kinase. Furthermore, immunohistochemistry using paraffin-embedded tissues from 62 patients showed not only that the frequency of recurrence was correlated with the plectin expression but that the prognosis of patients with a high plectin was extremely poor. Moreover, the survival rate of patients with a high plectin was significantly lower than that of patients with low E-cadherin levels, which is known to correlate with the poor prognosis of HNSCC. Our findings suggest that plectin promotes the migration and invasion of HNSCC cells through activation of Erk 1/2 kinase and is a potential prognostic biomarker of HNSCC.

1. Introduction

Head and neck squamous cell carcinoma (HNSCC) is the sixth most common cancer in the world, with a 5-year overall survival rate of approximately 40–50% [1,2]. Despite the improvement of therapies involving surgery, radiotherapy and chemotherapy, the prognosis of HNSCC patients in advanced stages is poor for local tumor recurrence and distant

* *Corresponding author at:* Laboratory of Proteome Research, National Institute of Biomedical Innovation, 7-6-8 Saito-Asagi, Ibaraki City, Osaka 567–0085, Japan. Tel.: +81 72 641 9811; fax: +81 72 641 9821.
E-mail address: tomonaga@nibio.go.jp (T. Tomonaga).

1874-3919/$ – see front matter © 2011 Elsevier B.V. All rights reserved.
doi:10.1016/j.jprot.2011.12.018

metastasis [3]. Most prognosis factors fail to provide definitive information regarding the biological behavior of the tumor and its recurrence and metastasis potential. Identifying a biomarker that correlates with recurrence and metastasis would provide more accurate information on prognosis and enable a more aggressive therapy to be selected for high-risk patients.

Proteomic technologies have been used to identify cancer-specific proteins that are useful for cancer diagnosis, prognosis, and therapeutic targets in HNSCC [4]. Although extensive proteome analysis has identified numerous proteins overexpressed in various cancer tissues, very few markers have become available for routine clinical use, mainly because potential candidates have not been detected due to their low abundance and/or validated extensively by other methods [5]. Two-dimensional difference gel electrophoresis methods (2D-DIGE) have been developed to overcome this problem [6-8]. We have previously identified several novel proteins with altered expression in colorectal, esophageal and liver cancers using this method [6-9].

In this study, we aimed to identify novel biomarkers to predict the clinical outcome of HNSCC patients. Using agarose 2D-DIGE, we compared protein expressions between head and neck cancer tissues and non-cancer tissues. Among several proteins identified to be differentially expressed between cancer and non-cancer tissues, we found that plectin is involved in the migration and invasion of HNSCC cells and is a novel prognostic marker for HNSCC.

2. Materials and methods

2.1. Human tissue samples and cell lines

Tissues from 12 patients with primary HNSCC were resected surgically without any neo-adjuvant therapy in the Department of Otorhinolaryngology, Head and Neck Surgery, Chiba University Hospital (Table 1). The ethics committee of the Graduate School of Medicine, Chiba University approved the protocol. Written informed consent was obtained from each patient before surgery. Excised samples were obtained within 60 min after the operation and were immediately placed in liquid nitrogen and stored at −80 °C. A human HNSCC-derived cell line D562 was obtained from the Human Science Research Resources Bank (Osaka, Japan). Cell lines were grown in IMDM with 10% FBS.

Table 1 – Clinical features of patients with HNSCC.

Sample number	Age	Gender	Location	UICC TN	UICC stage
1	66	Female	Hypopharynx	T4aN0	IVA
2	72	Male	Hypopharynx	T2N3	IVB
3	71	Male	Hypopharynx	T1N0	I
4	60	Male	Hypopharynx	T3N2c	IVA
5	69	Male	Hypopharynx	T3N2c	IVA
6	62	Male	Hypopharynx	T2N1	III
7	52	Female	Hypopharynx	T4aN2b	IVA
8	60	Male	Hypopharynx	T2N2c	IVA
9	81	Female	Hypopharynx	T4aN2b	IVA
10	74	Female	Hypopharynx	T4aN2b	IVA
11	66	Male	Hypopharynx	T4aN2b	IVA
12	64	Male	Hypopharynx	T4aN2b	IVA

2.2. Protein extraction and proteomic analysis

Protein extraction, agarose 2D-DIGE and enzymatic in-gel digestion of proteins were performed as described previously [7,8]. To identify proteins, digested peptides were injected into a trap column: 0.3×5 mm L-trap column (Chemicals Evaluation and Research Institute, Saitama, Japan), and an analytical column: 0.1×50 mm monolith column (AMR, Tokyo, Japan), which was attached to the Chorus 220 HPLC system (AMR). Purified peptides were introduced from HPLC to Q-star pulser i (Applied Biosystems, Foster City, CA, USA) at 500 nL/min. The MASCOT search engine (version 2.0.5, Matrixscience, London, UK) was used to identify proteins from the mass and tandem mass spectra of peptides. Peptide mass data were matched by searching the National Center for Biotechnology Information Human database (NCBInr 20080210, February 2008, 199851 entries). Database search parameters were: the charge (z) of the precursor ion, 2+ and 3+; peptide mass tolerance, 1.2 Da; fragment tolerance, 0.5 Da; enzyme was set to trypsin, allowing up to one missed cleavage; variable modifications, methionine oxidation. The minimum criterion of the probability-based MASCOT/MOWSE score was set with 5% as the significant threshold level. We considered >1.5 in spot volume to be significant according to previous reports as follows. Data set of all spots volumes obtained from six Cy3/Cy5 same sample showed robust thresholds of −2.33 and +1.52 for 90% confidence [10]. Furthermore, based on the observation that 2 S.D. ranged from 1.31 to 1.52, gel features changing by >1.5 in spot volume were considered significant [11].

2.3. Western blotting and immunohistochemistry

Western blotting (WB) and immunohistochemistry (IHC) were performed as described previously [7,8]. Anti-plectin goat polyclonal antibody (Santa Cruz Biotechnology Inc., Santa Cruz, CA) diluted 1:500 for WB and 1:50 for IHC, anti-periplakin rabbit polyclonal antibody (Bethyl Laboratories, Montgomery, TX) diluted 1:2000 for WB and 1:200 for IHC, anti-envoplakin mouse monoclonal antibody (Santa Cruz Biotechnology Inc.) diluted 1:1000 for WB and 1:100 for IHC, anti-cornulin (CRNN) rabbit polyclonal antibody (Proteintech Group, Chicago, IL) diluted 1:3000 for WB and 1:300 for IHC, and anti-β-actin goat polyclonal antibody (Santa Cruz Biotechnology Inc.) diluted 1:500 in blocking buffer were used as primary antibodies. Anti-integrin β4 antibody (Santa Cruz Biotechnology Inc.) diluted 1:50, and anti-E-cadherin antibody (Santa Cruz Biotechnology Inc.) diluted 1:50 were used for IHC.

All slides were examined by two of the authors (KK and TT) who were blinded to the clinical data. When the results were discordant, the judgment was made by the other investigator. Staining intensity was recorded on the following scale: 0, no staining is observed, or cytoplasm staining is observed in less than 10% of the tumor cells; 1+, faint/barely perceptible cytoplasm staining is detected in more than 10% of tumor

cells (the cells exhibit incomplete cytoplasm staining); 2+, weak or moderate cytoplasm staining is observed in more than 10% of tumor cells or strong cytoplasm staining in less than 30%; and 3+, strong cytoplasm staining is observed in more than 30% of tumor cells (Fig. S1). For statistical analysis, these categories were pooled (0 and 1+, "low"; 2+ and 3+, "high". Positive and negative control slides were included in all experiments.

2.4. *Gene knockdown using siRNA*

The target sequences for plectin RNA interference were as follows: plectin siRNA1: 5'-CCA AGA ACT TGC AGA AGT T-3', plectin siRNA2: 5'-CTG AGA ACC GCG CAC TCA T-3' purchased from Sigma Aldrich Japan (Tokyo, Japan).

2.5. *Cell proliferation assay*

D562 HNSCC cells in 24-well plates were transfected with siRNA (20nM final concentration). Both attached and floating cells were corrected with trypsinization. After staining with Trypan blue, the number of Trypan blue-positive cells was counted on days 2, 4, 6 after transfection.

2.6. *Wound healing assay*

Cell migration ability was evaluated by a wound healing assay. D562 cells were plated in 12-well dishes at a density of $2x10^6$ cells and transfected with siRNA (20nM final concentration). After overnight incubation, an artificial wound was carefully created at 0 h using a 200μl pipette tip to scratch the confluent cell monolayer. A photomicrograph was taken immediately after scratching (time 0 h) and 6 h and 24 h later.

2.7. *Matrigel invasion assay*

The invasion assay was carried out using the BioCoat Matrigel Invasion Chamber kit (Becton Dickinson Bioscience, Bedford, MA) according to the manufacturer's instructions. D562 cells were harvested, resuspended in FBS-free IMDM and seeded in a Matrigel invasion chamber or a control insert (2×10^5 cells/well). Lower chambers were filled with culture medium containing 10% FBS as a chemoattractant. After dispersed cells were cultured at 37 °C for 22 h, cells on the upper side of the membrane were then removed using a cotton swab and the filters were washed, fixed and stained using the Diff-Quick kit (Sysmex, Kobe, Japan). Percent invasion was represented as mean number of cells invading through a Matrigel insert membrane relative to that passing through a control insert membrane.

2.8. Statistical analysis

All data were analyzed using the statistical software SPSS11.0 for Windows. Overall survival was analyzed by the Kaplan-Meier method and the results were compared by log-rank test. Univariate analysis was performed for the correlation between overall survival time and various clinical characteristics, including gender, age, WHO histological type, clinical stage, and the expression levels of plectin, integrin β4 and E-cadherin. The significance of variables for survival was analyzed by the Cox proportional hazards model in multivariate analysis. The χ^2 test and Student's t test were used to compare clinicopathologic data. Statistical significance was assumed when <0.05.

3. Results

3.1. *Identification of differentially expressed proteins in human HNSCC tissue*

To identify novel markers useful for the diagnosis or prognosis of HNSCC, we used the agarose 2D-DIGE method to compare the profiling of protein expression between adjacent normal epithelial tissues (Cy3) and HNSCC tissues (Cy5) with

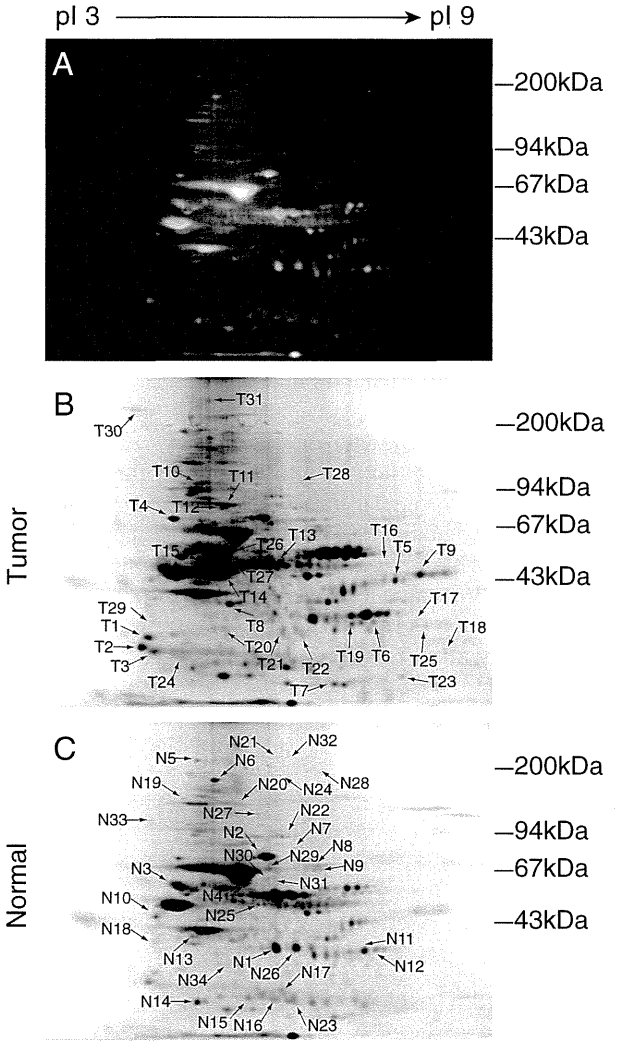

Fig. 1 – Proteomic analysis of HNSCC tissues using agarose 2-D DIGE. A, Increased protein spots in cancer tissues are displayed in red (Cy5), and decreased protein spots in cancer tissues in green (Cy3). B and C, conventional agarose 2-DE patterns of HNSCC (B) and non-cancer (C) were visualized by CBB staining.

a mixed-sample internal standard (Cy2) (Fig. 1A). Protein spots that were increased or decreased in tumor tissues were displayed as red or green, respectively. These spots were detected and quantitated with DeCyder imaging analysis software, and then statistical analysis was performed across the 12 gels. All of the samples were examined in duplicate or triplicate, and about 2500 protein spots (minimum 2297 and maximum 2518) were detected consistently in each gel. We considered >1.5 in spot volume to be significant as described in Material and Methods. The fluorescence volumes of 39 spots increased and 60 spots decreased in cancer tissues compared with adjacent normal epithelial tissues (Student's *t* test, $p<0.05$). To identify proteins, 300 μg protein in whole-cell lysate was separated by conventional agarose 2-DE and proteins were visualized by Coomassie blue staining (Fig. 1B, C). Of 99 spots, 88 (65 proteins) were identified by mass spectrometry (Table 2, 3, Fig. S2). Heat shock 27 kDa protein 1 was identified in both up-regulated (T27) and down-regulated proteins (N15) in HNSCC with a distinct pI value, which suggests that the protein was differently modified, probably phosphorylated, in cancer and normal tissues.

3.2. *Validation of the identified proteins by Western blotting and immunohistochemistry*

Among the 65 proteins with altered expression, we mainly focused on proteins, whose expression levels have not been well studied in head and neck cancers. The expression level of the four proteins (periplakin, envoplakin, cornulin, and plectin) with commercially available antibodies was examined by Western blotting. As shown in Fig. 2A, periplakin, envoplakin, and cornulin were significantly down-regulated in HNSCC tissues, whereas plectin was up-regulated, which confirms the results of proteomic analysis. The relative expression levels of plectin normalized with β-actin level are indicated below the Western blotting image. Although the same amount of protein was loaded in each lane, the expression level of β-actin was different in some of the cancer and normal tissue pairs, which might reflect the different expression of β-actin in these tissues.

Although there was no bias in the cellularity of normal and tumor tissues, whole tissue sections included non-epithelial components, and the altered protein expression in our 2D-DIGE analysis may have resulted from non-epithelial components. Thus, differential protein expression in HNSCC was validated by immunohistochemistry to examine the localization of identified proteins. Immunohistochemical validation studies were performed on paraffin-embedded samples from patients with cancer tissues and non-cancer tissues using four antibodies (plectin, periplakin, envoplakin, and cornulin). Although no staining of plectin was observed in normal squamous cells, tumor cells showed uniform staining in the cytoplasm and cell membrane (Fig. 2B). Periplakin, envoplakin and cornulin all showed strong and uniform staining in the cytoplasm of normal squamous cells; in particular, the horny layer and granular layer were strongly stained by anti-cornulin antibody. In marked contrast, faint, weak staining of proteins was observed in tumor cells (Fig. 2B). Examination of several tissue sections showed similar staining patterns, which indicates that altered expression of these proteins reflects actual changes in the protein level in cancer cells and not in stromal cells.

3.3. *Plectin knockdown inhibits proliferation, migration, and invasion of HNSCC cell lines*

Using proteomic analysis, we confirmed that several proteins were differentially expressed in HNSCC tissues. Among them, only plectin was upregulated, which could be a suitable biomarker for the diagnosis of HNSCC. Thus, we concentrated on plectin and investigated the functional role of plectin in HNSCC development.

First, we examined if plectin contributes to cell proliferation in HNSCC using the RNAi technique. After introduction of plectin siRNA into D562 cells for 48 hr, suppression of plectin was confirmed by Western blotting (Fig. 3A), while GL2 siRNA had no substantial effect on endogenous plectin expression. Then, the proliferation of D562 cells was examined by cell counting 2–6 days after siRNA treatment. As a result, cell proliferation was significantly reduced by plectin knockdown (Fig. 3B).

Penetration of the extracellular matrix and basement membrane by cancer cells is a key step in tumor invasion. Moreover, cell migration is essential for the invasion of cancer cells. Since plectin is a cross-linking protein of intermediate filaments, microtubules and actin microfilaments, it could be involved in tumor cell migration and invasion. In fact, plectin interacts with integrin β4, which has been reported to correlate with migration and invasion in HNSCC [12-14]. We therefore examined if plectin contributes to such cellular processes.

The effect of plectin knockdown on the migration potency of HNSCC cells was determined using the scratch-wound healing assay. The extent of wound closure can be taken as a direct measure of cell motility or migration capacity. Closure of the wound was almost complete in D562 cells carrying control siRNA within 24 hr of transfection, but the wound still existed in D562 cells into which plectin siRNA had been introduced. Thus, cell motility was significantly suppressed by plectin knockdown (Fig. 3C,D).

Next, the effect of plectin knockdown on HNSCC cell invasion was examined using the Matrigel invasion assay. Mock cells and plectin knockdown cells passed similarly through a control insert (Fig. 3E, upper), but the number of cells passing through the Matrigel insert membrane was markedly reduced in plectin knockdown invasive cells as compared with mock invasive cells (Fig. 3E, lower). Percent invasion of plectin siRNA-treated cells was significantly lower than that of mock or control siRNA-treated cells (Fig. 3F); therefore, a reduced level of endogenous plectin resulted in inhibited cell invasion in the HNSCC cell line.

3.4. *Phosphorylated Erk 1/2 decreases in plectin knockdown HNSCC cells*

What is the mechanism of the inhibition of migration and invasion in plectin knockdown HNSCC cells? A previous report by Osmanagic-Myers et al. showed that plectin−/− keratinocytes migrate faster than plectin+/+ cells, which is contrary to our results [15]. They showed that basal phosphorylation

Table 2 – Protein increased in HNSCC.

Protein increased in tumor tissue												
Spot no. [a]	Database accession no.	Unit ProtKB accession no.	Protein name	Average mass	Score	Seq. cov. (%) [b]	MS/MS (unique) [c]	Fold increase	Standard deviation	t-test	Pretension mass	References [e]
T1	gi-4507651	P67936	Tropomyosin 4	28,504	147	14	4	1.98	0.95	<0.001	33,000	(1)
T2	gi-187302	P31947	Epithelial cell marker protein 1	27,759	152	19	5	2.57	2.26	<0.001	31,000	(1,2)
T3	gi-49119653	P63104	YWHAZ protein	29,929	191	18	4	1.50	0.30	<0.001	31,000	(2)
T4	gi-16507237	P11142	Heat shock 70 kD protein 5	72,288	683	28	18	1.57	0.78	0.096	85,000	(3)
T5	gi-1199487	P50454	Collagen binding protein 2	46,506	245	22	8	4.54	1.95	<0.001	46,000	
T6	gi-45604447	P22626	Heterogeneous nuclear ribonucleoprotein A2/B1	35,984	145	14	3	2.01	1.00	0.015	34,000	
T7	gi-4505591	Q06830	Perox iredoxin 1	22,096	116	22	4	1.85	0.81	<0.001	23,000	(4)
T8	gi-62738525	P36952	Serpin	42,615	328	26	8	1.65	1.04	0.042	40,000	(5)
T9	gi-4503471	P68104	Eukaryotic translation elongation factor 1 alpha 1	50,109	215	11	5	5.39	2.79	<0.001	47,000	
T10	gi-42544159	Q92598	Heat shock 105 kD	96,804	329	10	8	1.52	0.56	0.028	110,000	
T11	gi-4504165	P06396	Gelsolin	85,644	286	10	6	1.52	0.41	0.018	90,000	(7)
T12	gi-10863945	P13010	ATP-dependent DNA helicase II	82,652	201	12	7	2.56	1.64	<0.001	880,000	
T13	gi-4507115	Q16658	Fascin 1	54,496	104	7	3	2.41	2.07	0.004	51,000	(8)
T14	gi-5031573	P61158	Actin-related protein 3	47,341	148	11	4	4.90	4.66	0.008	48,000	(8)
T15	gi-4503445	P19971	Endothelial cell growth factor 1 precursor	49,924	486	25	12	2.67	1.41	0.014	51,000	
T16	gi-30130	P50454	Collagen	46,238	97	6	2	3.25	2.74	0.013	47,000	(9)
T17	gi-75517570	P09651	HNRPA 1 protein	29,368	306	33	7	2.50	1.71	0.025	33,000	
T18	gi-181967	P68104	Elongation factor 1-alpha	35,205	52	3	1 [d]	1.93	1.00	0.075	32,000	
T19	gi-49168580	P40926	MDH2	35,537	613	46	15	3.02	4.53	0.031	34,000	
T20	gi-4557032	P07195	Lactate dehydrogenase B	36,615	213	20	6	1.53	0.54	0.006	33,000	
T21	gi-18645167	P07355	Annexin A2	38,552	177	18	5	4.57	5.05	<0.001	3200	(10)
T22	gi-37724561	P63244	Lung cancer oncogene 7	37,865	181	11	3	3.03	4.85	0.016	32,000	
T23	gi-48255905	Q01995	Transgelin	22,596	151	29	5	2.60	1.55	<0.001	25,000	
T24	gi-4504517	P04792	Heat shock 27 kDa protein 1	22,768	261	31	5	1.57	0.34	<0.001	30,000	(1)
T25	gi-47939618	P09651	Heterogeneous nuclear ribonucleoprotein A1	34,159	202	13	4	6.48	7.41	<0.001	32,000	
T26	gi-31542947	P10809	Chaperonin	61,016	496	34	16	2.08	1.70	0.01	62,000	(11)
T27	gi-31542947	P30101	ER0-60 protease	56,761	427	23	14	1.83	0.87	0.044	60,000	
T28	gi-320200	Q00839	Scaffold attachment factor A	90,423	427	11	8	2.59	1.37	0.009	120,000	
T29	gi-63252900	P09493	Tropomyosin 1 alpha chain	32,856	205	20	7	2.59	1.80	0.025	33,000	(11)
T30	gi-68533131	Q4LE33	TNC variant protein	244,248	2222	20	41	3.98	1.91	0.009	250,000	
T31	gi-41322908	Q15149	Plectin 1	513,393	503	5	20	1.69	0.64	0.035	30,000	

[a] Spot numbers refer to those in Fig. 1.
[b] Amino acid sequence coverage for the identified protein.
[c] Number of peptide fragments of a protein that yielded informative MS/MS data (number of unique peptide). The minimum criterion of the probability-based MASCOT/MOWSE score was set with 5% as the significant threshold level
[d] MS/MS spectrum refers to Fig. S2.
[e] The references are listed in Supplementary Information 3.

Table 3 – Protein decreased in HNSCC.

Protein decreased in tumor tissue												
Spot no. [a]	Database accession no.	Unit ProtKB accession no.	Protein name	Average mass	Score	Seq. cov. (%) [b]	MS/MS (unique) [c]	Fold decrease	Standard deviation	*t*-test	Pretension mass	References [d]
N1	gi-4502101	P04083	Annexin I	38,690	336	21	8	7.49	7.59	<0.001	39,000	(12)
N2	gi-4557871	P02787	Transferrin	77,000	259	11	7	5.13	3.07	<0.001	83,000	(13)
N3	gi-177831	P01009	Alpha-1-antitrypsin	46,677	252	21	8	6.18	4.08	<0.001	66,000	(2)
N4	gi-7706635	Q9UBG3	Cornulin	53,502	244	18	5	7.10	6.06	<0.001	66,000	(3)
N5	gi-179106	Q13813	Nonerythroid alpha-spectrin	284,107	648	11	24	1.81	0.81	0.014	220,000	
N6	gi-2992541	O60437	Periplakin	204,580	975	22	35	4.32	3.02	<0.001	182,000	
N7	gi-27436946	P02545	Lamin A/C	74,095	450	21	13	2.16	1.18	<0.001	81,000	(14)
N8	gi-119589476	P01024	Complement component 3	143,619	347	9	9	2.81	1.83	0.005	70,000	
N9	gi-37267	P29401	Transketolase	67,751	169	11	6	4.05	4.11	0.016	68,000	
N10	gi-340219	P08670	Vimentin	53,681	382	29	14	2.15	1.96	0.005	48,000	
N11	gi-40647126	P01860	Anti-HIV-1 gp120 immunoglobulin	22,899	54	11	2	4.96	5.15	0.014	52,000	(1,2)
N12	gi-12798841	P25705	ATP synthase	59,671	100	6	3	5.18	5.32	0.038	53,000	(11)
N13	gi-297412	P35237	Thrombin inhibitor	42,559	69	6	2	2.61	1.75	0.008	43,000	
N14	gi-178775	P02647	Propolipoprotein	28,944	187	21	5	4.58	2.14	<0.001	25,000	
N15	gi-4504517	P04792	Heat shock 27 kDa protein 1	22,768	279	33	7	1.72	0.62	<0.001	31,000	(1)
N16	gi-149673887	P01834	Immumoglobulin lights chain	23,331	109	17	2	2.44	1.15	<0.001	30,000	(1)
N17	gi-4502517	P00915	Carbonic annhydrase I	28,852	249	31	7	2.41	1.25	0.016	32,000	(2)
N18	gi-34234	P08865	Laminin-binding protein	31,774	141	14	3	5.16	10.01	0.004	44,000	(2)
N19	gi-87196339	P12109	Collagen type VI, alpha 1 precursor	108,462	319	10	9	3.52	5.06	<0.001	120,000	
N20	gi-41350923	P12110	Collagen type VI, alpha 2	108,539	151	5	4	3.43	4.91	0.026	120,000	
N21	gi-1147813	P15924	Desmoplakin I	331,571	190	3	7	2.45	2.08	0.043	220,000	(15)
N22	gi-4503483	P13639	Eukaryotic translation elongation factor 2	95,277	91	3	3	4.23	5.40	0.042	97,000	(15)
N23	gi-136066	P060174	Triosephosphate isomerase	26,609	432	38	7	2.58	1.60	<0.001	30,000	
N24	gi-14194715	Q92817	Envoplakin	231,477	110	1	2	2.52	2.24	0.007	20,0000	
N25	gi-860986	P07237	Protein disulfide-isomerase	56,644	141	8	5	2.10	1.63	0.061	47,000	(13)
N26	gi-13489087	P30740	Serine proteinase inhibitor	42,715	427	34	11	3.37	2.84	<0.001	41,000	(14)
N27	gi-4507877	P18206	Vinculin	116,649	177	6	7	1.93	0.71	<0.001	100,000	
N28	gi-55743104	P12111	Alpha 3 type VI collagen precursor	321,987	421	5	17	2.05	1.55	0.013	190,000	
N29	gi-5729877	P11142	Heat shock 70 kDa protein 8	70,854	156	7	4	4.76	4.74	0.004	62,000	(3)
N30	gi-386785	P08107	Heat shock protein	69,825	462	19	12	3.14	2.46	0.005	61,000	
N31	gi-157671915	Q6ZN66	Guarrylate binding protein 6	72,381	65	3	2	2.85	1.71	0.002	61,000	(3)
N32	gi-61743954	Q09666	AHNAK nucleoprotein	628,699	323	3	15	2.44	1.98	0.014	260,000	
N33	gi-124731	P07476	AHNAK nucleoprotein	68,427	218	15	7	2.16	1.35	0.003	115,000	
N34	gi-492570004	P13928	Annexin A8	36,872	69	6	2	3.66	2.71	0.035	35,000	(2)

[a] Spot numbers refer to those in Fig. 1.

[b] Amino acid sequence coverage for the identified protein.

[c] Number of peptide fragments of a protein that yielded informative MS/MS data (number of unique peptide). The minimum criterion of the probability-based MASCOT/MOWSE score was set with 5% as the significant threshold level.

[d] The references are listed in Supplementary Information 3.

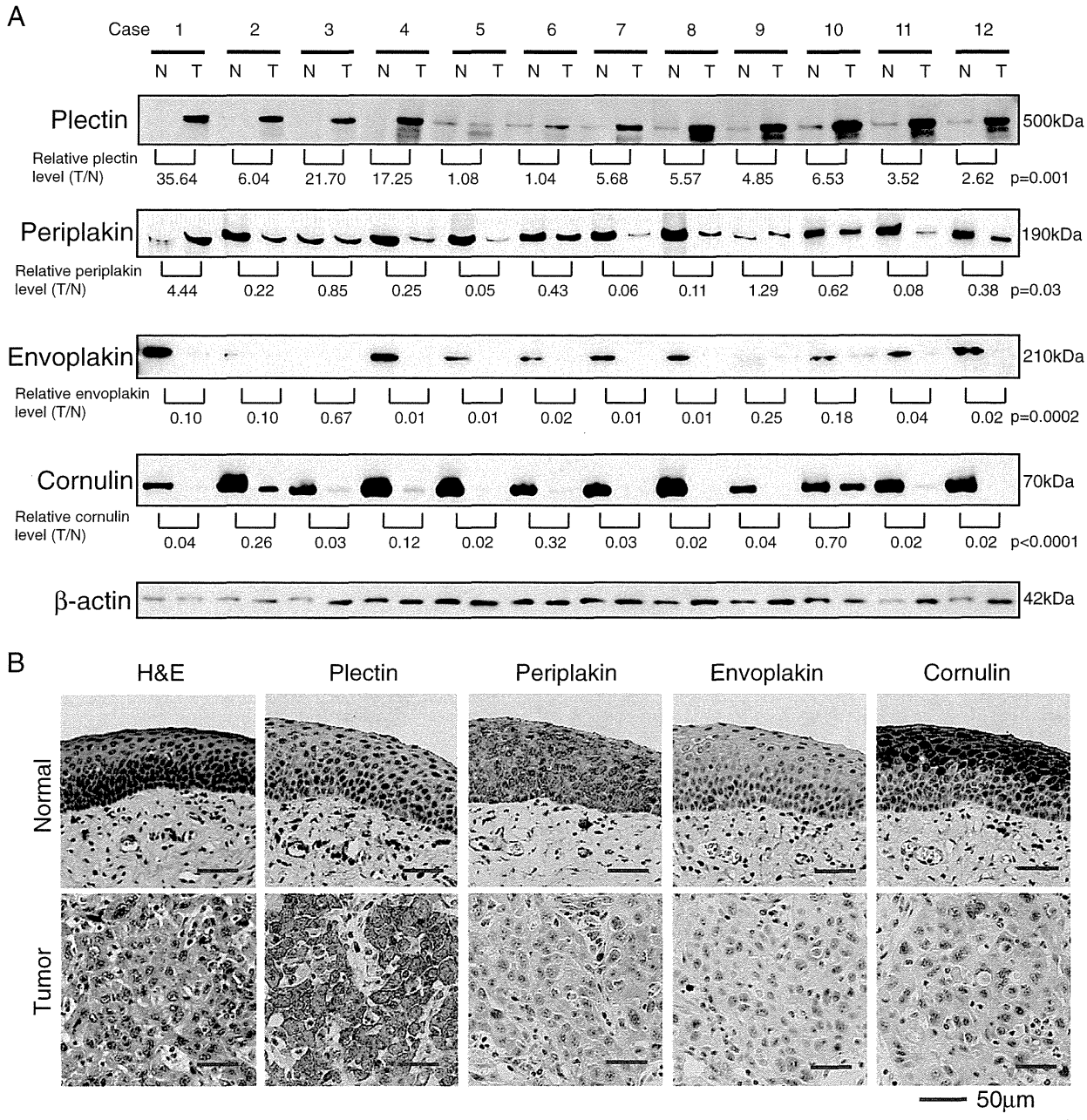

Fig. 2 – Validation of differentially expressed proteins in HNSCC tissues by Western blotting and immunohistochemistry. A, Western blots of total protein lysates prepared from twelve matched samples of tumor (T) and adjacent non-tumor tissue (N) with anti-plectin, anti-periplakin, anti-envoplakin, anti-cornulin, and anti-β-actin antibodies (loading control). The intensity of each band was measured with TotalLab™ 1D software (Nonlinear Dynamics, Newcastle upon Tyne, UK), and protein levels were calculated between tumor and non-tumor tissue, normalized with β-actin. The difference in protein expressions between (T) and (N) was assessed by Student's t-test for unpaired values. B, Immunohistochemical analysis of paraffin-embedded normal epithelia and cancer tissues with plectin, periplakin, envoplakin, and cornulin antibodies. HE: hematoxylin and eosin.

of Erk 1/2 kinases was significantly elevated in plectin−/− keratinocytes and was the cause of the faster migration of plectin-deficient cells. Upregulation of Erk 1/2 kinases has been shown to play a role in tumor invasion by inducing EMT [16], or by promoting the degradation of extracellular matrix proteins through induction of MMPs [17,18]. Furthermore, overexpression of N-cadherin induces cell migration in vitro and invasion and metastasis in vivo by an Erk 1/2-dependent mechanism [19,20]; therefore, we investigated Erk 1/2 activities in plectin knockdown HNSCC cells. Surprisingly, phosphorylated Erk 1/2 was significantly decreased in plectin siRNA-treated cells as compared with control siRNA-treated

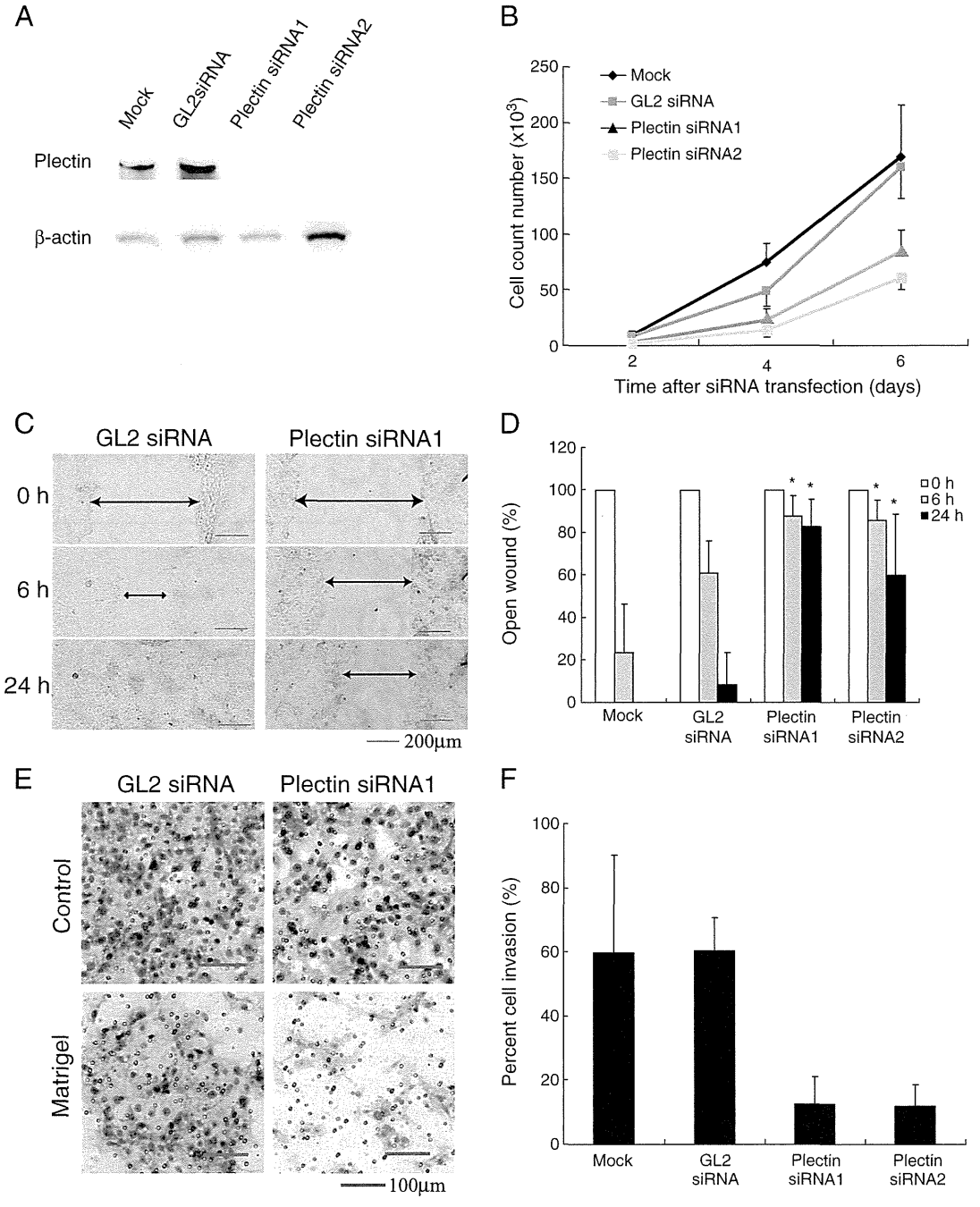

Fig. 3 – Suppression of plectin inhibits the cell proliferation, migration, and invasion of HNSCC cells. A, Expression of plectin in D562 cells was determined by Western blotting 24 hrs after plectin siRNA treatment. GL2 siRNA was used as a control. β-actin was used as a control for internal protein loading. B, Knockdown of plectin expression by siRNA significantly suppresses the proliferation of D562 cells. Cells were transfected with Mock, GL2siRNA, plectin siRNA1 and −2. Cells were cultured for the indicated time. *, $P<0.05$, control siRNA compared with siRNAs. C and D, Suppression of plectin decreased cancer cell migration. Cells were scratched with a pipette tip and migration toward the wounded area was observed. *, $P<0.05$, control siRNA compared with plectin siRNA. E, Suppression of plectin decreased cancer cell invasion. Representative images show cells that passed through the control chamber or Matrigel when transfected with control and plectin siRNA1. F, Three randomly selected fields were photographed and the number of invaded cells was counted. Percent cell invasion was calculated as the mean number of cells passing through a Matrigel insert membrane relative to passing through a control insert membrane. *, $P<0.05$, control siRNA compared with plectin siRNAs.

cells (Fig. 4A,B). Total Erk 1/2 level was also slightly decreased in plectin siRNA-treated cells (Fig. 4A,B). Although the relationship between plectin expression and Erk 1/2 activity remains obscure, these results suggest that the inhibition of migration and invasion in plectin knockdown cells may be associated with downregulation of Erk 1/2 kinase activities,

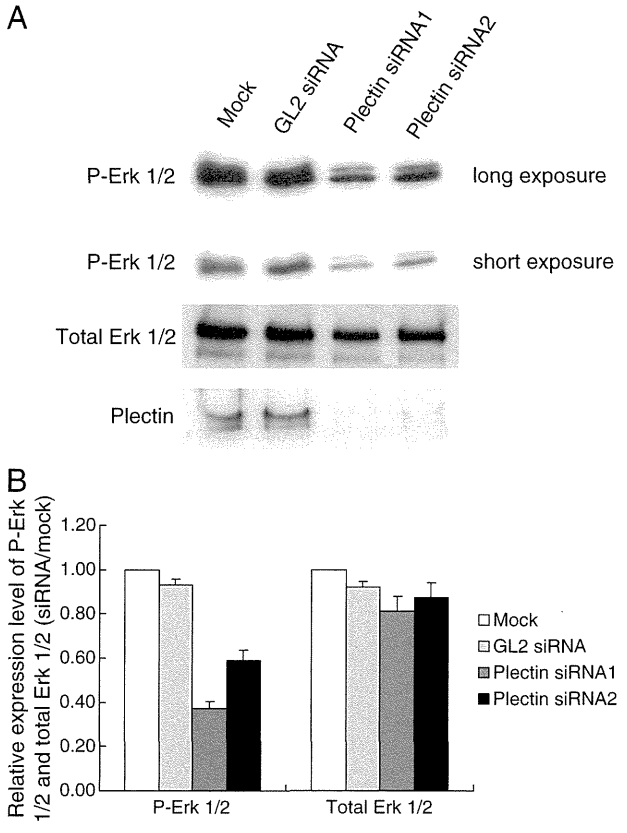

Fig. 4 – Suppression of plectin attenuates phosphorylated Erk 1/2 level. A. Expression of phosphorylated Erk 1/2 (P-Erk 1/2) and total Erk 1/2 in D562 cells was examined by Western blotting 24 hrs after plectin siRNA treatment. GL2 siRNA was used as a control. B. The intensity of P-Erk 1/2 and total Erk 1/2 bands in siRNA-treated cells were measured with TotalLab TL120 and the relative expression levels of each protein as compared with mock treatment are shown.

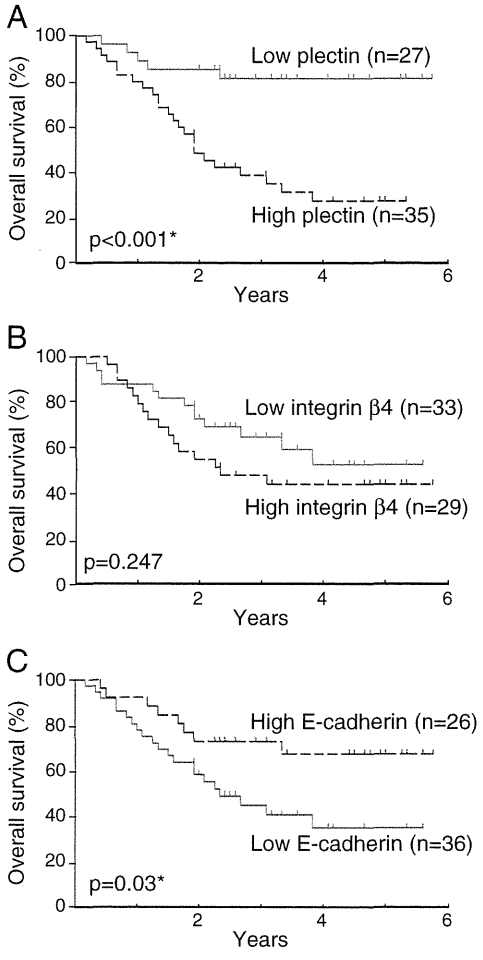

Fig. 5 – Kaplan-Meier survival curves according to expression levels of plectin (P<0.001; A), integrin β4 (P=0.247; B), and E-cadherin (P=0.03; C) in HNSCC.

which explains the different migration behavior between plectin-deficient keratinocytes and HNSCC cells.

3.5. *Plectin is a potential prognostic marker of HNSCC*

The above experiments strongly imply that upregulation of plectin is involved in metastasis and, as a result, the malignant potential of HNSCC. For this reason, we next examined whether plectin is associated with the prognosis of HNSCC patients. Immunohistochemistry of paraffin-embedded tissues obtained from 62 HNSCC patients was performed using anti-plectin antibody and its expression level was judged on a scale of 0 to 3+: 0, no staining; 1+, weak staining; 2+, moderate staining; 3+, strong staining (Fig. S1A). For statistical analysis, scores of 0 and 1+ were rated as low expression, and scores of 2+ and 3+ were rated as high expression. Survival curves were calculated by the Kaplan-Meier method and analyzed using the log-rank test. Strikingly, the survival rate of patients with a higher plectin level (≥2+) was significantly decreased ($P<0.001$) (Fig. 5A).

To test if the correlation of the survival rate and plectin expression level is comparable to other well-known prognosis markers of HNSCC, we analyzed the survival rate according to the expression levels of integrin β4 and E-cadherin, which were previously reported to correlate with the clinical outcomes of HNSCC patients [21-24]. Integrin β4 and E-cadherin expression levels were examined by IHC and judged on a scale of 0 to 3+ according to the intensity of staining (Fig. S1B, C). The results showed that a high expression of integrin β4 was not correlated with the poor prognosis of HNSCC patients ($P=0.247$, log-rank test) (Fig. 5B). Moreover, although a low expression of E-cadherin was correlated with the poor prognosis of HNSCC patients ($P=0.03$, log-rank test), its P value was much higher than that of statistical analysis by plectin expression (Fig. 5C). These results strongly indicate that plectin is a promising prognostic marker for HNSCC.

We further investigated whether the expression levels of plectin, integrin β4, and E-cadherin in cancer cells correlated with the clinical outcomes of HNSCC patients (Table 4). There was no significant correlation between plectin, integrin β4, or E-cadherin expression and gender, age, location of tumors, histology, clinical stage, or local recurrence; significant correlation was only observed between the plectin expression level and with or without distant metastasis in HNSCC patients. This result further supports the idea that plectin is involved in the metastasis and malignant potential of HNSCC.

Table 4 – Characteristics of 62 HNSCC patients in IHC analysis.

		Plectic-IHC expression			Integrin β4-IHC expression			E-cadherin-IHC expression		
	Total (62)	Low (27)	High (35)	P	Low (33)	High (29)	P	Low (36)	High (26)	P
Gender										
Male	50	21	29		27	23		31	19	
Female	12	6	6	NS	6	6	NS	5	7	NS
Age										
≧60	39	17	22		23	16		22	17	
<60	23	10	13	NS	10	13	NS	14	9	NS
Location of tumors										
Oral	23	11	12		14	9		12	11	
Oropharynx	2	1	1		1	1		2	0	
Hypopharynx	29	12	17		12	17		16	13	
Larynx	6	2	4		5	1		4	2	
Salivary gland	2	1	1	NS	1	1	NS	2	0	NS
Histology										
Well	18	10	8		12	6		7	11	
Moderate	38	14	24		19	20		26	12	
Poorly	6	3	3	NS	3	3	NS	3	3	NS
UICC-Stage										
I-III	17	10	7		12	5		9	8	
VI	45	17	28	NS	21	24	NS	27	18	NS
Local recurrence										
Yes	11	3	8		5	6		8	3	
No	51	24	27	NS	28	23	NS	28	23	NS
Distant metastasis										
Yes	25	7	18		14	11		15	10	
No	37	20	17	0.042	19	18	NS	21	16	NS

*Significance value $P<0.05$
NS, not significant

3.6. *Plectin is an independent prognostic marker of HNSCC*

Finally, we analyzed whether the plectin expression level was an independent clinical outcome factor in HNSCC patients. On univariate analysis, the clinical stage, plectin expression and E-cadherin expression were correlated with the overall survival time (Table 5, left). Furthermore, among these factors, the clinical stage (hazard ratio, 3.403; 95% confidence interval, 1.024–11.309, $P=0.0456$), plectin expression (hazard ratio, 5.519; 95% confidence interval, 1.653–18.433, $P=0.0055$) and E-cadherin expression (hazard ratio, 0.418; 95% confidence interval, 0.184–0.950, $P=0.0373$) were independent clinical outcome factors on multivariate analysis (Table 5, right). The data strongly suggested that plectin alone might be a prognostic biomarker of HNSCC.

4. Discussion

In this study, we searched for proteins that could serve as biomarkers for cancer diagnosis, prognosis, and therapeutic targets in HNSCC by agarose 2D-DIGE using surgically resected clinical specimens, and succeeded in identifying and validating several proteins that were differentially expressed in HNSCC. Among them, plectin was significantly overexpressed in HNSCC. Strikingly, HNSCC patients with a high plectin level suffered recurrence more frequently than those with a low plectin expression; as a result, the survival rate of patients with a high plectin level significantly declined. Furthermore, functional studies implied that a decreased expression of plectin suppresses the proliferation, migration and invasion of HNSCC cells. This is probably due to the downregulation of Erk 1/2 kinase activity in the cells, although whether it is caused by attenuated expression of plectin or by some other mechanism is unclear. These results provided evidence that plectin is a novel and promising prognostic biomarker of HNSCC.

Our results indicated that patients with a higher plectin level showed a much lower overall survival rate than those with a lower plectin level (Fig. 5). This difference in the survival rate is probably related with the higher metastatic potential of HNSCC with an increased plectin level (Table 4), which was supported by our experimental data and previous studies indicating that plectin is involved in cell migration and invasion. We showed that the suppression of endogenous plectin inhibited the migration and invasion of HNSCC cells (Fig. 3). In other studies, ablation of plectin impaired the migration of MCF-7 (human breast adenocarcinoma cell line) epithelial sheets [25]. Moreover, plectin interacts with the integrin β4, a receptor for laminins, which is a major component of the epidermal basement membrane [26]. Integrin β4 has been reported to associate with cell migration and invasion [12-14]. Furthermore, its high expression is associated with poor prognosis in a variety of human cancers [27,28]. Thus, overexpression of plectin might contribute to cell migration and invasion in HNSCC cells through its association with integrin β4.

On the other hand, Osmanagic-Myers et al. showed opposite results that suppression of plectin accelerates the

Table 5 – Prognostic factors by univariate and multivariate analysis.

Variables	Univariate analysis		Multivariate analysis	
	Hazard ratio 95% confidence interval	P	Hazard ratio 95% confidence interval	P
Gender (Male/Female)	0.608 (0.211-1.750)	0.3560		
Age (<60/≥60)	1.087 (0.505-2.340)	0.8312		
Location of tumors (larynx, pharynx/others)	0.494 (0.218-1.122)	0.0921		
WHO histological type (poor-moderate/well)	2.402 (0.913-6.325)	0.0759		
Clinical stage (I-III/VI)	4.471 (1.351-14.801)	0.0142*	3.403 (1.024-11.309)	0.0456*
Plectin (high/low)	6.359 (1.918-21.078)	0.0025*	5.519 (1.653-18.433)	0.0055*
Integrin β4 (high/low)	1.538 (0.739-3.204)	0.2498		
E-cadherin (low/high)	0.416 (0.184-0.942)	0.0355*	0.418 (0.184-0.950)	0.0373*

*Significance value $P<0.05$.

migration of keratinocytes [15]. How can this contradiction be explained? In keratinocytes, a MAP kinase Erk 1/2, which is known to positively regulate keratinocyte migration [29], was activated when plectin was depleted. This result was in marked contrast with our result that phosphorylated Erk 1/2 was down-regulated in plectin-deficient HNSCC cells. Ding et al. also reported that knockdown of plectin with RNA interference (RNAi) attenuates the activation of Erk1/2 in HEK293 cells [30]. The above results suggest that the effect on migration in plectin-deficient cells depends on the different response of Erk 1/2 activity to the alteration of plectin expression in each cell line.

Another mechanism of plectin-mediated migration and invasion might be its association with CXCR4 through the plectin N-terminal domain [30]. CXCR4 is the chemokine receptor for SDF-1 and has been reported to not only be expressed in a wide variety of carcinomas [31-34], but to be correlated with distant metastasis and poor prognosis in HNSCC [35]. Moreover, SDF-1/CXCR4 interaction is known to be involved in cell proliferation, migration, and invasion evoked through Erk 1/2 in several cancer cells [36-40]. This interaction and signal system may be related to the poor prognosis of HNSCC with high plectin expression.

We also observed that suppression of plectin inhibited the proliferation of HNSCC cells (Fig. 3), which suggests that plectin is involved in cancer development. In fact, overexpression of plectin has been previously reported in prostate cancer, colorectal cancer, and pancreatic cancer [41-43], although the precise mechanism of how plectin overexpression is related to cancer development is not clear. Plectin is a large protein that links intermediate filaments to microtubules and microfilaments, anchoring the cytoskeleton to the plasma and nuclear membranes [44,45]. It also plays important roles in signal transduction, is involved in Rho/Rac/Cdc42 signaling cascades [46] and is an early substrate for caspase 8 following apoptosis induction by CD95 or tumor necrosis factor receptor [47]. Thus, upregulation of plectin in HNSCC may have an impact on the signaling pathways that regulate cell migration and apoptosis.

Postoperative adjuvant therapy for HNSCC is now applied on the basis of the results of pathological examination of the surgical specimens (multiple lymph node metastases, extralymphatic invasion, a positive stump after microscopic resection). Efficacy of chemoradiotherapy as compared with radiotherapy alone was evaluated in two randomized trials conducted in Europe (European Organization Research and Treatment of Cancer; EORTC) and the United States (Radiation Therapy Oncology Group; RTOG) [48,49]. Although EORTC study revealed that chemoradiotherapy significantly increased overall survival without a high incidence of adverse effects, RTOG trial showed not only a marginal improvement of overall survival but significant increase in severe adverse effects with chemoradiotherapy. Inconsistencies emerged from these reports emphasizes an intense need to define more precise boundaries demarcating risk levels for the decision-making processes of adjuvant treatment [50]. Therefore, while chemotherapy combined with radiotherapy are effective as postoperative adjuvant therapies for HNSCC, better biomarkers to select patients with proper indications are necessary to practically improve the clinical outcome of the patients and/or prevent a risk of adverse effects of the treatment. In this regard, plectin could be a useful biomarker for more effective postoperative treatment options, such as radiation alone for patients with a low plectin level and radiation in combination with chemotherapy for patients with a high plectin level.

In summary, we identified plectin as a promising prognostic biomarker in HNSCC, which could make significant contributions to the prediction of HNSCC patient prognosis and might improve their clinical outcome through postoperative follow-up and additional therapy. Further investigation is needed to uncover the mechanisms responsible for plectin-mediated development of HNSCC.

Supplementary materials related to this article can be found online at doi:10.1016/j.jprot.2011.12.018.

Disclosure

The authors declare no conflicts of interest.

Acknowledgments

We would like to thank Masumi Ishibashi and Takahiro Kazami for their technical assistance. This work is supported

by Grants-in-Aid 18014007, 18659363, 19390330, 20014003 to T.T and 19390154 to F.N from the Ministry of Education, Science, Sports and Culture of Japan.

REFERENCES

[1] Jemal A, Siegel R, Ward E, Hao Y, Xu J, Thun MJ. Cancer statistics, 2009. CA Cancer J Clin 2009;59:225–49.

[2] Gold KA, Lee HY, Kim ES. Targeted therapies in squamous cell carcinoma of the head and neck. Cancer 2009;115:922–35.

[3] Hardisson D. Molecular pathogenesis of head and neck squamous cell carcinoma. Eur Arch Otorhinolaryngol 2003;260:502–8.

[4] Yarbrough WG, Slebos RJ, Liebler D. Proteomics: clinical applications for head and neck squamous cell carcinoma. Head Neck 2006;28:549–58.

[5] Srinivas PR, Verma M, Zhao Y, Srivastava S. Proteomics for cancer biomarker discovery. Clin Chem 2002;48:1160–9.

[6] Tomonaga T, Matsushita K, Yamaguchi S, Oh-Ishi M, Kodera Y, Maeda T, et al. Identification of altered protein expression and post-translational modifications in primary colorectal cancer by using agarose two-dimensional gel electrophoresis. Clin Cancer Res 2004;10:2007–14.

[7] Nishimori T, Tomonaga T, Matsushita K, Oh-Ishi M, Kodera Y, Maeda T, et al. Proteomic analysis of primary esophageal squamous cell carcinoma reveals downregulation of a cell adhesion protein, periplakin. Proteomics 2006;6:1011–8.

[8] Seimiya M, Tomonaga T, Matsushita K, Sunaga M, Oh-Ishi M, Kodera Y, et al. Identification of novel immunohistochemical tumor markers for primary hepatocellular carcinoma; clathrin heavy chain and formiminotransferase cyclodeaminase. Hepatology 2008;48:519–30.

[9] Wu D, Matsushita K, Matsubara H, Nomura F, Tomonaga T. An alternative splicing isoform of eukaryotic initiation factor 4H promotes tumorigenesis in vivo and is a potential therapeutic target for human cancer. Int J Cancer 2011;128: 1018–30.

[10] Karp NA, Kreil DP, Lilley KS. Determining a significant change in protein expression with DeCyder during a pair-wise comparison using two-dimensional difference gel electrophoresis. Proteomics 2004;4:1421–32.

[11] Hu Y, Malone JP, Fagan AM, Townsend RR, Holtzman DM. Comparative proteomic analysis of intra- and interindividual variation in human cerebrospinal fluid. Mol Cell Proteomics 2005;4:2000–9.

[12] Mercurio AM, Rabinovitz I, Shaw LM. The alpha 6 beta 4 integrin and epithelial cell migration. Curr Opin Cell Biol 2001;13:541–5.

[13] Lipscomb EA, Mercurio AM. Mobilization and activation of a signaling competent alpha6beta4integrin underlies its contribution to carcinoma progression. Cancer Metastasis Rev 2005;24:413–23.

[14] Mercurio AM, Rabinovitz I. Towards a mechanistic understanding of tumor invasion–lessons from the alpha6beta 4 integrin. Semin Cancer Biol 2001;11:129–41.

[15] Osmanagic-Myers S, Gregor M, Walko G, Burgstaller G, Reipert S, Wiche G. Plectin-controlled keratin cytoarchitecture affects MAP kinases involved in cellular stress response and migration. J Cell Biol 2006;174:557–68.

[16] Janda E, Lehmann K, Killisch I, Jechlinger M, Herzig M, Downward J, et al. Ras and TGF[beta] cooperatively regulate epithelial cell plasticity and metastasis: dissection of Ras signaling pathways. J Cell Biol 2002;156:299–313.

[17] Chakraborti S, Mandal M, Das S, Mandal A, Chakraborti T. Regulation of matrix metalloproteinases: an overview. Mol Cell Biochem 2003;253:269–85.

[18] Whyte J, Bergin O, Bianchi A, McNally S, Martin F. Key signalling nodes in mammary gland development and cancer. Mitogen-activated protein kinase signalling in experimental models of breast cancer progression and in mammary gland development. Breast Cancer Res 2009;11:209.

[19] Hazan RB, Phillips GR, Qiao RF, Norton L, Aaronson SA. Exogenous expression of N-cadherin in breast cancer cells induces cell migration, invasion, and metastasis. J Cell Biol 2000;148:779–90.

[20] Hulit J, Suyama K, Chung S, Keren R, Agiostratidou G, Shan W, et al. N-cadherin signaling potentiates mammary tumor metastasis via enhanced extracellular signal-regulated kinase activation. Cancer Res 2007;67:3106–16.

[21] Kurokawa A, Nagata M, Kitamura N, Noman AA, Ohnishi M, Ohyama T, et al. Diagnostic value of integrin alpha3, beta4, and beta5 gene expression levels for the clinical outcome of tongue squamous cell carcinoma. Cancer 2008;112:1272–81.

[22] Mattijssen V, Peters HM, Schalkwijk L, Manni JJ, van 't Hof-Grootenboer B, de Mulder PH, et al. E-cadherin expression in head and neck squamous-cell carcinoma is associated with clinical outcome. Int J Cancer 1993;55: 580–5.

[23] Bowie GL, Caslin AW, Roland NJ, Field JK, Jones AS, Kinsella AR. Expression of the cell-cell adhesion molecule E-cadherin in squamous cell carcinoma of the head and neck. Clin Otolaryngol Allied Sci 1993;18:196–201.

[24] Takes RP, Baatenburg De Jong RJ, Alles MJ, Meeuwis CA, Marres HA, Knegt PP, et al. Markers for nodal metastasis in head and neck squamous cell cancer. Arch Otolaryngol Head Neck Surg 2002;128:512–8.

[25] Boczonadi V, McInroy L, Maatta A. Cytolinker cross-talk: periplakin N-terminus interacts with plectin to regulate keratin organisation and epithelial migration. Exp Cell Res 2007;313:3579–91.

[26] Rezniczek GA, de Pereda JM, Reipert S, Wiche G. Linking integrin alpha6beta4-based cell adhesion to the intermediate filament cytoskeleton: direct interaction between the beta4 subunit and plectin at multiple molecular sites. J Cell Biol 1998;141:209–25.

[27] Chao C, Lotz MM, Clarke AC, Mercurio AM. A function for the integrin alpha6beta4 in the invasive properties of colorectal carcinoma cells. Cancer Res 1996;56:4811–9.

[28] Lu S, Simin K, Khan A, Mercurio AM. Analysis of integrin beta4 expression in human breast cancer: association with basal-like tumors and prognostic significance. Clin Cancer Res 2008;14:1050–8.

[29] Huang C, Jacobson K, Schaller MD. MAP kinases and cell migration. J Cell Sci 2004;117:4619–28.

[30] Ding Y, Zhang L, Goodwin JS, Wang Z, Liu B, Zhang J, et al. Plectin regulates the signaling and trafficking of the HIV-1 co-receptor CXCR4 and plays a role in HIV-1 infection. Exp Cell Res 2008;314:590–602.

[31] Kaifi JT, Yekebas EF, Schurr P, Obonyo D, Wachowiak R, Busch P, et al. Tumor-cell homing to lymph nodes and bone marrow and CXCR4 expression in esophageal cancer. J Natl Cancer Inst 2005;97:1840–7.

[32] Muller A, Homey B, Soto H, Ge N, Catron D, Buchanan ME, et al. Involvement of chemokine receptors in breast cancer metastasis. Nature 2001;410:50–6.

[33] Yasumoto K, Koizumi K, Kawashima A, Saitoh Y, Arita Y, Shinohara K, et al. Role of the CXCL12/CXCR4 axis in peritoneal carcinomatosis of gastric cancer. Cancer Res 2006;66:2181–7.

[34] Koshiba T, Hosotani R, Miyamoto Y, Ida J, Tsuji S, Nakajima S, et al. Expression of stromal cell-derived factor 1 and CXCR4 ligand receptor system in pancreatic cancer: a possible role for tumor progression. Clin Cancer Res 2000;6:3530–5.

[35] Katayama A, Ogino T, Bandoh N, Nonaka S, Harabuchi Y. Expression of CXCR4 and its down-regulation by IFN-gamma

in head and neck squamous cell carcinoma. Clin Cancer Res 2005;11:2937–46.
[36] Barbero S, Bonavia R, Bajetto A, Porcile C, Pirani P, Ravetti JL, et al. Stromal cell-derived factor 1alpha stimulates human glioblastoma cell growth through the activation of both extracellular signal-regulated kinases 1/2 and Akt. Cancer Res 2003;63:1969–74.
[37] Tan CT, Chu CY, Lu YC, Chang CC, Lin BR, Wu HH, et al. CXCL12/CXCR4 promotes laryngeal and hypopharyngeal squamous cell carcinoma metastasis through MMP-13-dependent invasion via the ERK1/2/AP-1 pathway. Carcinogenesis 2008;29:1519–27.
[38] Brand S, Dambacher J, Beigel F, Olszak T, Diebold J, Otte JM, et al. CXCR4 and CXCL12 are inversely expressed in colorectal cancer cells and modulate cancer cell migration, invasion and MMP-9 activation. Exp Cell Res 2005;310:117–30.
[39] Phillips RJ, Burdick MD, Lutz M, Belperio JA, Keane MP, Strieter RM. The stromal derived factor-1/CXCL12-CXC chemokine receptor 4 biological axis in non-small cell lung cancer metastases. Am J Respir Crit Care Med 2003;167:1676–86.
[40] Hwang JH, Hwang JH, Chung HK, Kim DW, Hwang ES, Suh JM, et al. CXC chemokine receptor 4 expression and function in human anaplastic thyroid cancer cells. J Clin Endocrinol Metab 2003;88:408–16.
[41] Nagle RB, Hao J, Knox JD, Dalkin BL, Clark V, Cress AE. Expression of hemidesmosomal and extracellular matrix proteins by normal and malignant human prostate tissue. Am J Pathol 1995;146:1498–507.
[42] Lee KY, Liu YH, Ho CC, Pei RJ, Yeh KT, Cheng CC, et al. An early evaluation of malignant tendency with plectin expression in human colorectal adenoma and adenocarcinoma. J Med 2004;35:141–9.
[43] Kelly KA, Bardeesy N, Anbazhagan R, Gurumurthy S, Berger J, Alencar H, et al. Targeted nanoparticles for imaging incipient pancreatic ductal adenocarcinoma. PLoS Med 2008;5:e85.
[44] Sonnenberg A, Liem RK. Plakins in development and disease. Exp Cell Res 2007;313:2189–203.
[45] Wiche G. Role of plectin in cytoskeleton organization and dynamics. J Cell Sci 1998;111(Pt 17):2477–86.
[46] Andra K, Nikolic B, Stocher M, Drenckhahn D, Wiche G. Not just scaffolding: plectin regulates actin dynamics in cultured cells. Genes Dev 1998;12:3442–51.
[47] Stegh AH, Herrmann H, Lampel S, Weisenberger D, Andra K, Seper M, et al. Identification of the cytolinker plectin as a major early in vivo substrate for caspase 8 during CD95- and tumor necrosis factor receptor-mediated apoptosis. Mol Cell Biol 2000;20:5665–79.
[48] Cooper JS, Pajak TF, Forastiere AA, Jacobs J, Campbell BH, Saxman SB, et al. Postoperative concurrent radiotherapy and chemotherapy for high-risk squamous-cell carcinoma of the head and neck. N Engl J Med 2004;350:1937–44.
[49] Bernier J, Domenge C, Ozsahin M, Matuszewska K, Lefebvre JL, Greiner RH, et al. Postoperative irradiation with or without concomitant chemotherapy for locally advanced head and neck cancer. N Engl J Med 2004;350:1945–52.
[50] Bernier J, Cooper JS, Pajak TF, van Glabbeke M, Bourhis J, Forastiere A, et al. Defining risk levels in locally advanced head and neck cancers: a comparative analysis of concurrent postoperative radiation plus chemotherapy trials of the EORTC (#22931) and RTOG (# 9501). Head Neck 2005;27:843–50.

uicc
global cancer control

IJC
International Journal of Cancer

An alternative splicing isoform of eukaryotic initiation factor 4H promotes tumorigenesis *in vivo* and is a potential therapeutic target for human cancer

Di Wu[1], Kazuyuki Matsushita[1], Hisahiro Matsubara[2], Fumio Nomura[1] and Takeshi Tomonaga[1,3]

[1] Department of Molecular Diagnosis (F8), Graduate School of Medicine, Chiba University, Chuo-ku, Chiba, Japan
[2] Department of Frontier Surgery (M9), Graduate School of Medicine, Chiba University, Chuo-ku, Chiba, Japan
[3] Laboratory of Proteome Research, National Institute of Biomedical Innovation, Ibaraki City, Osaka, Japan

Deregulation of protein synthesis plays a critical role in cell transformation. Several translation initiation factors (eIFs) have been implicated in malignant transformation; thus, suppression of eIFs could be a potential cancer therapy if cancer cells are selectively killed without damaging healthy cells. One of the potential molecular targets is a cancer-specific splicing variant. We have previously shown that one of the splicing variants of eIF4H (isoform 1) was overexpressed in primary human colorectal cancer. Our study aimed to explore whether eIF4H isoform 1 contributes to carcinogenesis and could be an efficient molecular target for human cancer therapy. We found that its overexpression in immortalized mouse fibroblasts, NIH3T3 cells, generated tumors in nude mice. Conversely, suppression of eIF4H isoform 1 expression using specific siRNA inhibited the proliferation of colon cancer cells *in vitro* and subcutaneously implanted tumor *in vivo*. Strikingly, eIF4H isoform 1 specific siRNA showed no effect on the growth of immortalized human fibroblasts. More interestingly, ectopic expression of eIF4H isoform 1 greatly increased the cyclin D1 level. On the other hand, cyclin D1 decreased by shRNA-mediated suppression of eIF4H isoform 1. Moreover, cotransfection of eIF4H isoform 1 siRNA and cyclin D1 expression plasmid was able to reverse the growth suppression effect of eIF4H isoform 1 knockdown. These results suggest that eIF4H isoform 1 plays an important role in carcinogenesis through the activation of oncogenic signaling and could be a promising molecular target for cancer therapy.

There is increasing evidence that deregulation of protein synthesis is associated with cell transformation and the malignant phenotype.[1–4] Protein synthesis is primarily regulated at the step of ribosome recruitment to the 5′-mRNA terminus and this association is mediated by a trimeric complex, termed eIF-4F, which consists of the large scaffolding protein eIF4G, the RNA helicase eIF4A, and the cap binding protein eIF4E. Several eIFs have been demonstrated to be involved in carcinogenesis. Overexpression of eIF4E, a subunit of the eIF-4F complex, has been observed in many solid tumors and tumor cell lines[1–5] and, in experimental models, it markedly alters cellular morphology, enhances proliferation and induces cellular transformation, tumorigenesis and metastasis.[6–8] Other members of the eIF-4F complex are also implicated in malignant transformation. For example, eIF4G is overexpressed in squamous cell lung carcinomas[9,10] and its overexpression in NIH3T3 cells leads to anchorage-independent growth of cells and tumor formation in nude mice.[11] eIF4A, an ATP-dependent RNA helicase, is also overexpressed in human melanoma cells and primary hepatocellular carcinomas.[12,13] eIF4H was first identified to stimulate translation in rabbit reticulocytes.[14] It has been recognized that eIF4H stimulates protein synthesis by enhancing the helicase activity of eIF4A by increasing the processivity of eIF4A.[14–16] We have previously reported that eIF4H was overexpressed in most human colorectal cancer tissues[17]; thus, it has become evident that control of mRNA translation plays a critical role in carcinogenesis. A likely mechanism of cellular transformation by eIFs has been suggested as increased translational efficiency of the mRNA responsible for the control of cell growth or

Key words: alternative splicing, translation initiation factor, therapeutic target

Abbreviations: CHAPS: 3-[(3-cholamidopropyl) dimethylammonio]-1-propanesulfonate; DTT: dithiothreitol; eIFs: eukaryotic initiation factors; FACS: fluorescence-activated cell sorting; IMDM: iscove's modified dulbecco's media; MTS: 3-(4, 5-dimethylthiazol-2-yl)-5-(3-carboxymethoxyphenyl)-2-(4-sulfophenyl)-2H-tetrazolium; RNAi: RNA interference; RPMI-1640: Roswell Park Memorial Institute media; shRNA: short hairpin RNA; TdT: terminal deoxynucleotidyl transferase; Tet-Off system: tetracycline-off system; TUNEL: terminal deoxynucleotidyl transferase-mediated dUTP nick end labeling assay

Additional Supporting Information may be found in the online version of this article.

Grant sponsor: Ministry of Education, Science, Sports and Culture of Japan; **Grant numbers:** 16390353, 17015007, 18058006, 19390330
DOI: 10.1002/ijc.25419
History: Received 2 Nov 2009; Accepted 12 Apr 2010; Online 27 Apr 2010

Correspondence to: Takeshi Tomonaga, Laboratory of Proteome Research, National Institute of Biomedical Innovation, 7-6-8 Saito-Asagi, Ibaraki City, Osaka 567-0085, Japan, Tel.: 81-72-641-9862, Fax: 81-72-641-9861, E-mail: tomonaga@nibio.go.jp

apoptosis, although the precise mechanism of how these factors are involved in carcinogenesis remains to be established.

Alternative splicing has been observed in many cancer-associated genes, suggesting that it might have a key role in carcinogenesis.[18–21] Hence, cancer-specific spliced isoforms may be potential tools as tumor markers or for molecular treatments that can be designed to recognize only the variant form. The *eIF4H* gene is known to produce two splice variants, isoform 1 and 2 (exon 5 is alternatively spliced),[22] which generate two protein products, 27 kDa and 25 kDa. Between them, overexpression of isoform 1 is much more prominent than isoform 2 in colon cancers. In this regard, eIF4H isoform 1 might be a cancer-driving splice variant and therefore a promising therapeutic target.

In our work, we investigated whether the alternative splicing form of eIF4H contributes to cell proliferation and carcinogenesis. We showed that overexpression of eIF4H isoform 1 induces tumor formation in nude mice and its suppression inhibited cell proliferation *in vitro* and *in vivo*. The effect of eIF4H isoform 1 on proliferation is likely due to the upregulation of an oncogenic factor cyclin D1. Our results suggest that eIF4H isoform 1 might become an attractive target of therapeutic intervention for colon cancer.

Material and Methods

Human tissue samples

Tissues from 10 patients with primary colorectal and 20 patients with esophageal cancer (Table 1) were resected surgically in the Department of Frontier Surgery, Chiba University Hospital. The ethics committee of the Graduate School of Medicine, Chiba University approved the protocol. Written informed consent was obtained from each patient before operation. The percentage of tumor cells in the tissues was 50–80% in all cases. The excised samples were obtained within 1 hr after the operation from tumor tissues and the corresponding nontumor tissues of the same patients 5–10 cm from the tumor. All excised tissues were placed immediately in liquid nitrogen and stored at −80°C until analysis.

Cell culture

Two human colon cancer cell lines, LOVO and RKO, two human lung fibroblast cell lines, MRC5 and WI38, and a mouse fibroblast, NIH3T3, were purchased from RIKEN Cell Bank (Tsukuba, Japan). The tumor cells, LOVO and RKO, were grown in RPMI-1640, and immortalized cells, MRC5, WI38 and NIH3T3, were grown in IMDM medium, both supplemented with 10% fetal bovine serum (FBS), 1% (v/v) penicillin and streptomycin (100 U/ml) (all from Invitrogen, Carlsbad, CA), and maintained at 37°C in a 5% CO_2-95% air atmosphere.

Real-time quantitative PCR

Total RNA was extracted from tumor and nontumor tissues with an RNeasy Mini kit (Qiagen, Tokyo, Japan). Total RNA from the nucleus and cytoplasm of colon cancer cells was extracted with a Protein and RNA Isolation System (PARIS) Kit (Applied Biosystems Japan, Tokyo, Japan). cDNA was synthesized from total RNA with the first-strand cDNA synthesis kit for RT-PCR (Roche, Mannheim, Germany). Real-time quantitative PCR of eIF4H cDNA using the LightCycler

Table 1. Clinical features of patients with esophageal cancer and colorectal cancer

No.	Age	Sex	Location	Stage[1]	Histological type
Patients with esophageal cancer					
1	66	M	Mt/Ut	2a	Mod[2]
2	53	M	Ae	3	Mod[2]
3	67	M	Mt/Ut	4b	Well[2]
4	64	M	Ae	2a	Mod[2]
5	55	M	Mt	2a	Mod[2]
6	56	M	Ut/Mt	4b	Mod[2]
7	67	M	Lt	1	Mod[2]
8	63	M	Mt/Lt	4b	Mod[2]
9	62	M	Lt	3	Well[2]
10	55	M	Lt	2a	Well[2]
11	73	M	Lt	4a	Mod[2]
12	63	M	Lt/Ae	3	Mod[2]
13	71	M	Lt/Ae	3	Mod[2]
14	63	M	Lt/Ae	4b	Well[2]
15	64	M	Mt	3	Mod[2]
16	45	M	Lt/Ae/Mt	4b	Poor[2]
17	54	M	Ae	4a	Mod[2]
18	54	M	Lt/Ae	3	Well[2]
19	58	M	Lt/Ae	2a	Combined[2]
20	67	M	Lt/Ae	2a	Mod[2]
Patients with colorectal cancer					
6R	57	M	S	2	Well[3]
27R	51	M	R	4	Mod[3]
29R	51	M	R	3b	Mod/Poor[3]
34R	59	M	R	3a	Well/Mod/Poor[3]
35C	72	F	S	2	Well[3]
36C	67	M	T	3a	Mod/Poor[3]
37C	49	M	R	3a	Well[3]
112	72	M	S	3b	Mod[3]
117	49	M	Ce	4	Mod[3]
118	85	M	S	2	Well[3]

[1]Stage is described according to Union Internationale Contre le Cancer (UICC) TNM Classification (Fifth Edition, 1997). [2]Well, well-differentiated squamous cell carcinoma; Mod, moderately differentiated squamous cell carcinoma; Poor, poorly differentiated squamous cell carcinoma; Combined, combined squamous cell carcinoma with basaloid carcinoma. [3]Well, well-differentiated adenocarcinoma; Mod, moderately differentiated adenocarcinoma; Poor, poorly differentiated adenocarcinoma.Abbreviations: Ut: upper thoracic esophagus; Mt: middle thoracic esophagus; Lt: lower thoracic esophagus; Ae: abdominal esophagus; S: sigmoid colon; R: rectum; T: transverse colon; Ce: cecum.

instrument (Roche) was carried out in 20 μl of reaction mixture containing 2 μl of 10× LightCycler DNA Master SYBR Green I (FastStart Taq DNA polymerase, deoxynucleotide triphosphate, buffer, SYBR Green I), 3.0 mM $MgCl_2$ and 0.5 μM each of forward (5′-GGAAGCCTTGACATACGAT-3′), and reverse primer (5′-CATCCCTGAAGCCAGAAT-3′) in a LightCycler capillary. Real-time quantitative PCR of cyclin D1 cDNA was carried out in 20 μl of reaction mixture containing 2 μl of 10× LC FastStart DNA Master Hybridization Probes, 4.0 mM $MgCl_2$ and 0.5 μM each of forward (5′-CCC CAA CAA CTT CCT GTC CTA-3′) and reverse primer (5′-CTC CAG CAG GGC TTC GAT-3′) 0.3 μM of Fluorescein Probe (5′-AGG CAG TCC GGG TCA CAC TTG ATC ACT-3′-Fluorescein), 0.4 μM of LCRed Probe (5′-LCRed640-5′-TGG AGA GGA AGC GTG TGA GGC GGT A-3′-phosphorylation) in a LightCycler capillary. Serial dilutions of template cDNA were made for PCRs to optimize PCR products within the linear range. LightCycler software version 3.3 (Roche) was used for analysis of quantitative PCR.

Western-blot analysis

Frozen tissue samples were solubilized in lysis buffer (7 M urea, 2 M thiourea, 2% 3-[(3-cholamidopropyl) dimethylammonio]-1-propanesulfonate (CHAPS), 0.1 M dithiothreitol (DTT), 2% IPG buffer (Amersham Pharmacia Biotech, Buckinghamshire, UK), 40 mM Tris) using a Polytron homogenizer (Kinematica, Switzerland) followed by centrifugation (100,000*g*) for 1 hr at 4°C. Cultured cells were solubilized in SDS sample buffer (62.5 mM Tris-Cl pH6.8, 2% SDS, 20% glycerol, 0.2% bromophenol blue, 0.025% β-mercaptoethanol) and heated for 5 min at 100°C. After passing through 27G needles, the samples were centrifuged for 15 min at 15,000*g*. A 30-μg sample of total protein from each lysate was loaded and separated by electrophoresis on 10–20% gradient gels (Bio-Rad, Hercules, CA). The proteins were transferred to polyvinylidene fluoride membranes (Millipore, Bedford, MA) in a tank-transfer apparatus (Bio-Rad), and the membranes were blocked with 5% skim milk in PBS. Antibodies used include eIF4H (prepared by Japan Bio Services, Saitama, Japan diluted 1:500), cyclin D1 (Sigma, Japan; 1:1,000), ornithine decarboxylase (ODC; Sigma; 1:200), Bcl-XL (Sigma; 1:1,000), Bcl-2 (Sigma; 1:1,000) and c-Myc (Oncogene Research Products, La Jolla, CA 1:500). Goat anti-rabbit IgG horseradish peroxidase (Bio-Rad) diluted 1:3,000, mouse anti-rabbit IgG horseradish peroxidase (Bio-Rad) diluted 1:1,000 and rabbit anti-goat IgG horseradish peroxidase (Cappel, West Chester, PA) diluted 1:500 in blocking buffer were used as secondary antibodies. Antigens on the membrane were detected with enhanced chemiluminescence detection reagents (Amersham Pharmacia Biotech).

Plasmid transfection and establishment of eIF4H isoform 1 overexpressed stable NIH3T3 Tet-Off cell line

The Tet-off system utilizes the tetracycline-dependent transcriptional repression activity of tTA protein (BD Biosciences Clontech, Palo Alto, CA). The eIF4H isoform 1 cDNA, driven by a tTA-repressible CMV promoter element in a TRE-Tight plasmid (pTRE-Tight/eIF4H isoform 1), was constructed as follows. Full-length eIF4H isoform 1 was amplified by PCR using HeLa cDNA library as a template and cloned into the TRE-Tight vector plasmid (BD Biosciences Clontech). Plasmids were purified with an Endofree® Plasmid Maxi Kit (Qiagen) and the DNA sequences were verified. To generate the NIH3T3 Tet-Off stable cell line, pTet-Off plasmid (BD Biosciences Clontech) was transfected as described previously.[23,24] Briefly, NIH3T3 cells were plated in 6-well plates in IMDM containing 10% FBS without antibiotics one day before transfection so that they were at 70–90% confluence at the time of transfection. On the day of transfection, 4 μg plasmids and 10 μl Lipofectamine 2000™ (Invitrogen) were diluted in 250 μl Opti-MEM I Reduced-Serum Medium (Invitrogen), respectively. After 5-min incubation at room temperature, the diluted plasmids and Lipofectamine 2000™ were combined and then further incubated for 20 min at room temperature. Then, DNA-Lipofectamine 2000™ complexes were then added to each well and cells were incubated for 48 hr at 37°C in a CO_2 incubator. NIH3T3 cells, 5×10^4, transfected with pTet-Off plasmid were transferred to 10-cm dishes 48 hr after transfection, and 400 μg/ml geneticin (Invitrogen) and 1 μg/ml doxycycline (Dox) were added to complete medium containing IMDM, 10% FBS, 1% penicillin-streptomycin. The complete medium with geneticin was replaced every 4 days and fresh Dox was added every 2 days until geneticin-resistant colonies began to appear. At least 30 clones were screened to find the clone with the highest induction in the absence of Dox and with the lowest background. Once the NIH3T3 Tet-Off stable cell line was obtained, the eIF4H isoform 1-overexpressed stable NIH3T3 Tet-Off cell line was generated by transfecting pTRE-Tight/eIF4H isoform 1 plasmid and linear hygromycin marker (0.2 μg) into the cells. Stable clones were selected by adding 400 μg/ml hygromycin and 1 μg/ml Dox to the medium as described above.

Gene knockdown using siRNA and cotransfection of cyclin D1 expression plasmid

siRNA targeting eIF4H RNA were generated to reduce eIF4H expression. The target sequence for eIF4H siRNA was 5′-AACCCACAGAAGAGGAAAGAG-3′ (si102), which is common to two splice variants of eIF4H, and two eIF4H isoform 1 specific siRNA were 5′-AATGGGTAGCTCTCGA GAATC-3′ (si103), 5′-AATCTAGAGGTGGATGGGATT-3′ (si104) (Japan Bio Services) and eIF4H isoform 2-specific siRNA was 5′-AUG ACA GAG GCU UCA GGG A-3′ (iGENE, Tokyo, Japan). Blast analysis (http://www.ncbi.nlm.nih.gov/BLAST/) did not reveal overlapping regions between target sequences and other human genes. Cyclin D1 expression plasmid (CCND1 Human cDNA Clone) was purchased from Origene (Rockville, MD). Transfection of siRNA and plasmid was performed using lipofectamin 2000™ as described above.

Establishment of eIF4H isoform 1 stable knockdown colon cancer cell line

The eIF4H shRNAs, siRNA oligonucleotides connected by a spacer sequence, were cloned into a pBAsi-hU6 Neo plasmid (Takara Bio; Japan), where eIF4H shRNAs were driven by a hU6 promoter. The resulting plasmids, pBAsi-hU6-eIF4H shRNAs, were then transfected into LOVO cells and eIF4H isoform 1 stable knockdown clones, sh103-1, sh103-2 and sh104, were selected by adding 400 μg/ml geneticin, as described above.

Proliferation assays

Viable cell number was assessed according to 3-(4,5-dimethylthiazol-2-yl)-5-(3-carboxymethoxyphenyl)-2-(4-sulfophenyl)-2H-tetrazolium (MTS) dye absorbance following the manufacturer's instructions (Promega, Madison, WI). Absorbance was measured using a Wallac 1420 ARVOsx Multilabel Counter (Perkin-Elmer, Tokyo, Japan). Experiments were repeated in eight parallel studies.

Cell cycle analysis

Cells were fixed in 70% ethanol and treated with 50 μg/ml propidium iodide (Wako, Japan) in the presence of 200 μg/ml RNase A. Then, cells were subjected to cell cycle analysis using fluorescence activated cell sorting (FACS) Caliber cytometer (Becton Dickinson, San Jose, CA). At least 10,000 cells were counted for each sample, and data were analyzed with a Cell Quest program (Becton Dickinson, San Jose, CA).

TUNEL assay

Apoptotic cells were detected by the TUNEL assay according to the manufacturer's instructions (Apoptosis Detection System, Fluorescein; Promega). Briefly, cells cultured in 6-well plate were fixed with paraformaldehyde at 4°C for 10 min on ice and permeabilized with 0.5% Triton-X-100 solution in PBS for 5 min. After washing with PBS twice, apoptotic cells were visualized through the detection of internucleosomal fragmentation of DNA using *in situ* nick-end labeling with terminal deoxynucleotidyl transferase (TdT) and FITC-labeled dUTP (MEBSTAIN Apoptosis Kit; Medical & Biological Laboratories, Japan).

Subcutaneous injection of the cells and tumor formation in nude mice

Male BALB/c nude mice, 4–5 weeks of age, were subcutaneously injected with 1×10^6 LOVO cells or 6×10^5 NIH3T3 cells into the left leg. Tumor size was calculated using the formula $(ab^2)/2$, where a and b represent the larger and smaller diameters, respectively, and was monitored every 3 days.

Results

eIF4H isoform 1 was overexpressed in gastrointestinal cancers

eIF4H gene is known to produce two splice variants, isoform 1 and 2 (exon 5 is alternatively spliced), which generate two protein products, 27 kDa and 25 kDa. Between them, not isoform 2, but isoform 1 expression, was significantly increased in colorectal cancers.[17] We then investigated if this was true in other gastrointestinal cancers, such as esophageal cancer. Detailed information on the esophageal cancer and colorectal cancer cases is shown in Table 1. Total protein lysates were prepared from 20 matched samples of the tumor (T) and adjacent nontumor tissue (N) and the expressions of eIF4H isoforms were examined with anti-eIF4H antibody. We found that eIF4H isoform 1 protein, but not isoform 2, was greatly increased in most esophageal cancers compared with the corresponding nontumor tissues (Figs. 1*a* and 1*b*), although there were no striking correlations between patient's pathological data and the eIF4H isoform 1 expression level (Table 1).

We therefore decided to focus on eIF4H isoform 1 in further studies. To examine if the increase of eIF4H isoform 1 occurred at the mRNA level, a set of primers that specifically amplifies isoform 1 was designed and real-time quantitative RT-PCR was carried out using total RNA extracted from tumor and nontumor tissues of 20 esophageal and 10 colorectal cancer patients (Fig. 1*c*). The eIF4H isoform 1 mRNA level was significantly elevated in the tumors, indicating that overexpression of the eIF4H isoform 1 is regulated at the mRNA level, such as elevated transcription, mRNA stability or de-regulation of alternative splicing.

Overexpression of eIF4H isoform 1 in NIH3T3 cell leads to tumor formation in nude mice

To directly investigate the transforming potential of eIF4H isoform 1, we created NIH3T3 cell lines that overexpress eIF4H isoform 1 using a Tet-Off gene expression system. The NIH3T3 cell line, which expresses the tetracycline-controlled transactivator, was stably trasfected with the eIF4H isoform 1 expression plasmid under the control of the tetracycline-responsive promoter so that eIF4H isoform 1 was expressed only in the absence of doxycycline (Dox). The cells were then screened for inducible eIF4H isoform 1 protein expression by immunoblotting with anti-eIF4H antibody. Three stable clones, no. 9, 10 and 306, were obtained, in which eIF4H isoform 1 expression was greatly induced by Dox removal from the media (Fig. 2*a*). Strikingly, subcutaneous injection of these stable clones overexpressing eIF4H isoform 1 into nude mice formed tumors after 3.5 weeks, whereas control mice injected with NIH3T3 cells did not generate tumors (Figs. 2*b* and 2*c*). These results suggest that eIF4H isoform 1 possesses transforming activity *in vivo*.

Suppression of eIF4H isoform 1 inhibits proliferation of colon cancer cell lines

To further examine the involvement of eIF4H isoform 1 in cell proliferation and carcinogenesis, RNA interference (RNAi) was used to suppress eIF4H expression. Several siRNA were designed to target different regions of the eIF4H open reading frame (Supporting Information Figure 1). Among them, siRNA (si103 and si104) suppressed only isoform 1

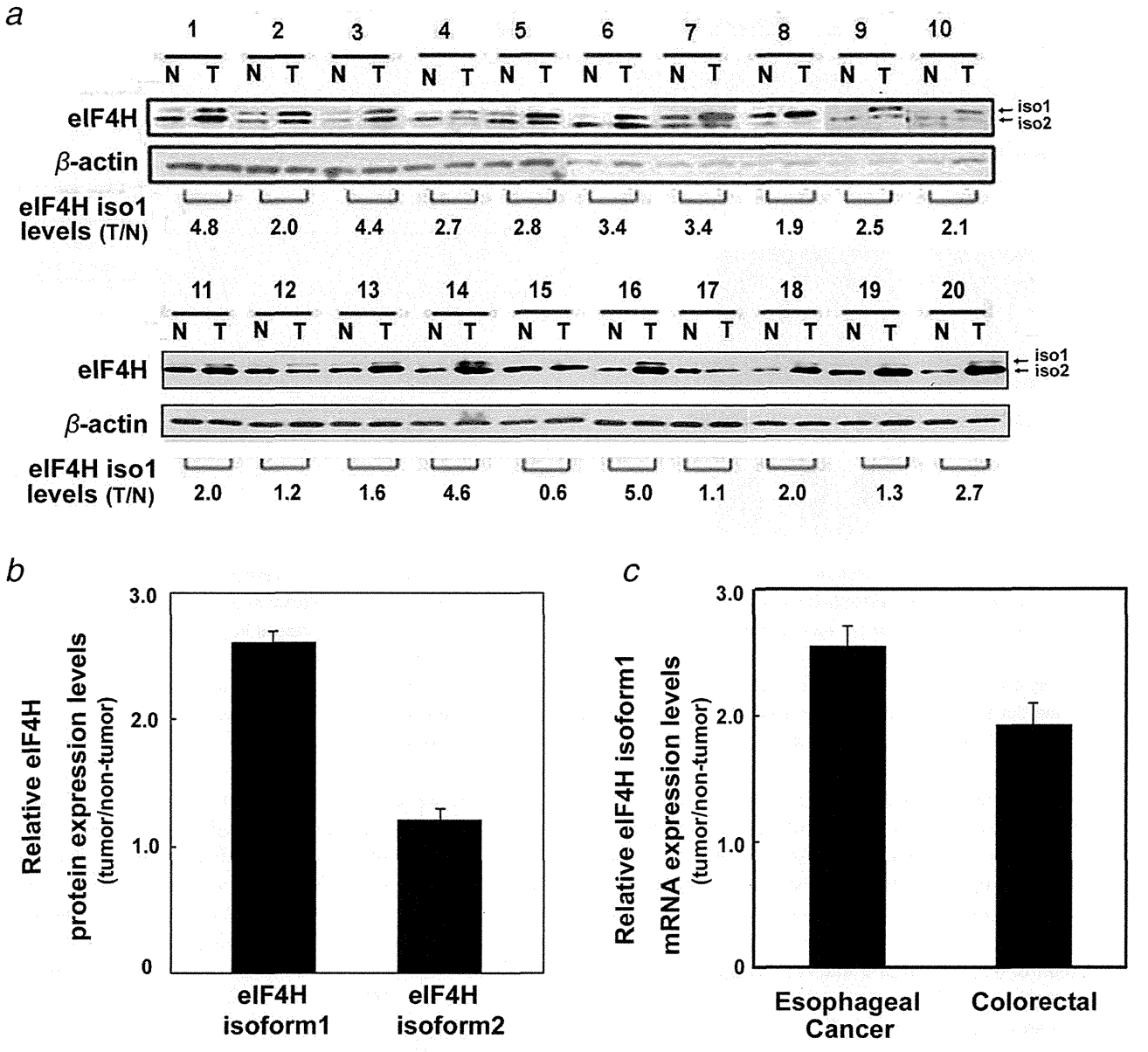

Figure 1. eIF4H isoform 1 was overexpressed in primary esophageal cancers tissues. (*a*) Total protein lysates were prepared from 20 matched samples of the tumor (T) and adjacent nontumor tissues (N). Equal amounts of protein from each pair were resolved on 10–20% gradient polyacrylamide gel and immunoblotted with anti-eIF4H and β-actin antibodies. Upper band: isoform 1; lower band: isoform 2. (*b*) The intensity of each band in (*a*) was measured with NIH Image and the mean ± SD of the relative eIF4H protein levels between tumor and nontumor tissue of 20 esophageal cancer patients normalized with β-actin were calculated. (*c*) Total RNA was prepared from matched samples of tumor and adjacent nontumor tissue of esophageal cancer and colorectal cancer patients, and real-time PCR was performed to examine the eIF4H isoform 1 mRNA level. Mean ± SD of relative eIF4H mRNA levels between tumor and nontumor tissue of 20 esophageal and 10 colorectal cancer patients normalized with β-actin were calculated.

and si201 suppressed only isoform 2 expression 48 hr after siRNA treatment in two colon cancer cell lines, LOVO and RKO (Figs. 3*a* and 3*b*); therefore, these three eIF4H siRNA (si103, 104 and 201) were used for further analysis.

To investigate the effect of eIF4H suppression on cell growth, the MTS assay was performed 48 hr after siRNA treatment of LOVO and RKO (Figs. 3*c* and 3*d*). Surprisingly, the suppression of eIF4H isoform 1 alone, using si103 and si104, strongly decreased the viable cell number by 30–50% as compared with the control. A similar decrease of the cell number was observed in RKO cells. These results imply that eIF4H isoform 1 plays an important role in the proliferation of colon cancer cells. Next, we examined if the suppression of eIF4H isoform 2 inhibits the proliferation of colon cancer